Title
Mechanistic Studies of Biomimetic Reactions by Synthetic Enzyme Mimics

Author
Hart-Cooper, William Michael

Publication Date
2015

Peer reviewed|Thesis/dissertation

Mechanistic Studies of Biomimetic Reactions by Synthetic Enzyme Mimics

By

William Michael Hart-Cooper

A dissertation submitted in partial satisfaction of the
requirements for the degree of
Doctor of Philosophy
in
Chemistry
in the
Graduate Division
of the
University of California, Berkeley

Committee in charge:
Professor Kenneth N. Raymond, Co-chair
Professor Robert G. Bergman, Co-chair
Professor Alexander Katz

Summer 2015

Abstract

Mechanistic Studies of Biomimetic Reactions by Synthetic Enzyme Mimics

By

William Michael Hart-Cooper

Doctor of Philosophy in Chemistry

University of California, Berkeley

Professor Kenneth N. Raymond, Co-chair

Professor Robert G. Bergman, Co-chair

Chapter 1. A brief introduction to common synthetic host structures and justification for the work described herein is provided.

Chapter 2. The development of 1 and related hosts as a new class terpene synthase mimics that catalyze intramolecular Prins cyclizations. The property of water exclusion is observed. Host 1 is also shown to compensate for the gem-disubstituent effect.

Chapter 3. The development of new terephthalamide hosts enabled an investigation of the effect of host structure on the enantio- and diastereoselectivity of these reactions, as well as a simple kinetic analysis. Rate accelerations and turnover numbers are notably high.

Chapter 4. The mechanism of proton transfer in an archetypal enzyme mimic is studied using amide hydrogen deuterium exchange (HDX) kinetics. Collectively, these data shed light on the role of acid, base and water-mediated proton transfer in a synthetic active site with relevance to proton-mediated catalysis. Moreover, the emergent mechanism of solvent-occupied proton transfer raises the prospect of designable hosts with properties that are unique to the integration of their parts

Chapter 5. A short overview is provided, which places the results of chapters 2-4 in context with some broader goals of biomimetic supramolecular chemistry.

Mechanistic Studies of Biomimetic Reactions by Synthetic Enzyme Mimics

Table of Contents

Acknowledgments

Graduate school gave me an appreciation for the depth and detail of a good molecular story, introduced me to the useful but limited nature of experiment and theory, and revealed the challenging art of reaching a valid conclusion. The past five years have been very enriching, and the lessons I've learned were a product of the exceptional people I've met here.

Ken always has a story or joke on hand and provides the group with endless encouragement, support, surprising leaps of intuition and a fundamentally sound repertoire of advice. Bob teaches us how to balance creativity and a big-picture vantage with organization, efficiency and scientific rigor. Dean constantly generates new ideas, sees through bad ones and manages to coherently interpret our explanations when we are at our least articulate, yet still is very relatable and treats his students as equals.

Casey introduced me to the lab and gave sound advice on what it means to be a graduate student, while showing the habits of an effective mentor. Tiffany and Tatum have been great friends, and nerding out with them over beers have led to sparkling conversations, strange ideas and the occasional hilarious dare. Allegra has been a fantastic buddy and I will miss our afternoon procrastination conversations. James and Ben have been great to work out with and I look forward to the interesting directions they take the BASIS school visits. Tommy impressed with his considerate nature, going so far as to rescue a parakeet from being eaten by a lizard. Kristen was great to chat with, a great collaborator and role model. Chen brought energy, enthusiasm and a stream of new results, and spreads these characteristics like a disease to those who work with him. The speed with which Lionel moved a project forward was impressive, even if he landed into the occasional English language-related misunderstanding. Derek is probably the most patient person I know, and a great mentor with sound advice. Ka king's surprise wedding made for an unforgettable Sunday-night bachelor party. Nicola has, and always will be, our resident expert in the field "quark synthesis," and was very kind and supportive to everyone he works with. It was a treat to collaborate with Lena on our fifth grade science lessons, the development of which she has a real talent for. Reba brought a huge source of energy and enthusiasm to the group. Rebecca, Dave and Cindy have impressed me with their achievements, intellectual growth and abilities to foster a positive and fun subgroup. I am excited to follow the directions that they will lead the cluster project in the coming years.

I owe so much to Mom, who has always helped me to follow my passions, even if it involves transforming our yard into a hobby farm and garage into a metallurgy workshop. Dad taught me how to build stuff, giving me the satisfaction and confidence that comes from making, by one's own design and hands, something totally new. Geoff has been the best older brother I could ask for, inventing the beloved childhood game "trapped in a box and rolled down the stairs," being a constant source of support and advice, and nudging me back on track academically at a crucial time during my teenage years. Making art, crafts and catching bugs with Emily is, and always will be, huge fun. Her optimism and creativity has been a great source of support, and I can't wait to see the impact she will have on her students. Patrick and I have shared some great adventures, and with each passing year, I am inspired by his initiative, passion, and self-propelled growth, both emotional and intellectual. Tammy has been a huge source of support and helped me grow more

than I ever would've predicted five years ago. Her encouragement, feedback and love have helped me through the hard times, and I am truly lucky to have her by my side.

Chapter 1
Synthetic Chemical Microenvironments

Introduction

Over the last two hundred years, chemists' understanding of small molecule covalent bonding and synthesis has matured. Recent advances in information technology have simultaneously increased individual productivity, accelerated the rate of knowledge production and facilitated intellectual ferment among scientists who, three decades ago, may seldom have come in contact. By iteratively building on the shoulders of predecessors, skilled chemists now routinely synthesize complex molecules previously existing only in exotic organisms.[1,2] With current methods, it is now possible to synthesize almost any structurally reasonable small molecule, albeit often without great efficiency. These methods have driven multidisciplinary advancements in every scientific field.

Sustained progress in molecular synthesis enables future generations of chemists to begin asking questions of timely and pressing relevance.[3] Can we construct nanoscale machines to harvest energy from the sun and more broadly, meet the chemical needs of the super-organism that is modern society? Can current chemical infrastructure be replaced in a responsible manner that allows our species to sustainably coexist with the environment? What is the hydrophobic effect and how does it drive the organization of matter? Are there molecular mechanisms by which organismal intelligence crystallizes? How do molecules organize themselves to become living cells and organisms—in chemical terms, what are we? Keys to addressing these questions lie in understanding the advanced chemistry of living organisms, which to a large degree, operates through the noncovalent interactions of polymeric macromolecules. Supramolecular chemistry, as the study of noncovalent interactions between molecules, is a chemical frontier where these questions are beginning to be addressed.

Nature has perfected nanoscale fabrication through trial, error and natural selection over the last four billion years. Synthetic chemists have long been enamored with the prospect of designing analogous customizable nanoenvironments.[4,5] One approach to this ambitious goal involves the development of cavity-containing host molecules that provide a separate phase from bulk solution. After molecular encapsulation, this microenvironment may endow a guest material with drastically different properties from those observed in bulk solvent. Chemists have developed these host cavities for selective molecular recognition, and less frequently, catalysis. The scientific motivation for this dissertation is to provide a small contribution to these two areas. A brief summary of some examples of artificial receptors and catalysts that were known before the work discussed in subsequent chapters was performed, and are illustrated in Figure

Cucurbiturils were named for the fruits they resemble (*Cucurbita pepo* i.e. pumpkin).[6] These macrocycles are formed by condensation between glycouril and formaldehyde and are among the first hosts inside which dramatically enhanced guest reactivity was observed, in the dipolar cycloaddition occurring between azide and alkyne.[7,8] This rate enhancement is presumably driven by ion-dipole interactions, which encourage enhanced rate by increasing the proximity between two reactive functionalities. However, catalytic turnover was limited by product inhibition. The structural variety of these hosts has been substantially expanded in recent years.[9,10] Exploiting the hydrophobic effect, host-guest shape and size complementarity and ion-dipole interactions, attomolar binding affinities have been observed. This affinity is the largest so far measured in synthetic hosts and surpasses the characteristically strong association of streptavidin and biotin.[11] If applied selectively to a transition state, this magnitude of stabilization could afford rate accelerations comparable to the most efficient of enzymes. Investigations into the catalytic use of cucurbiturils therefore remain promising.

Calixarenes are structurally versatile host molecules. A classic report describes using a calixarene-derived "carcerand" to stabilize the highly reactive cyclobutadiene molecule.[12] The four-fold rotational symmetry of resorcin[4]arene enables the formation of hydrogen-bonded hexameric cubic hosts, which catalyze acid-mediated reactions.[13,14] Given the variety and utility of this class of hosts, calixarene derivatives will continue to constitute an important class of noncovalent receptors and catalysts.

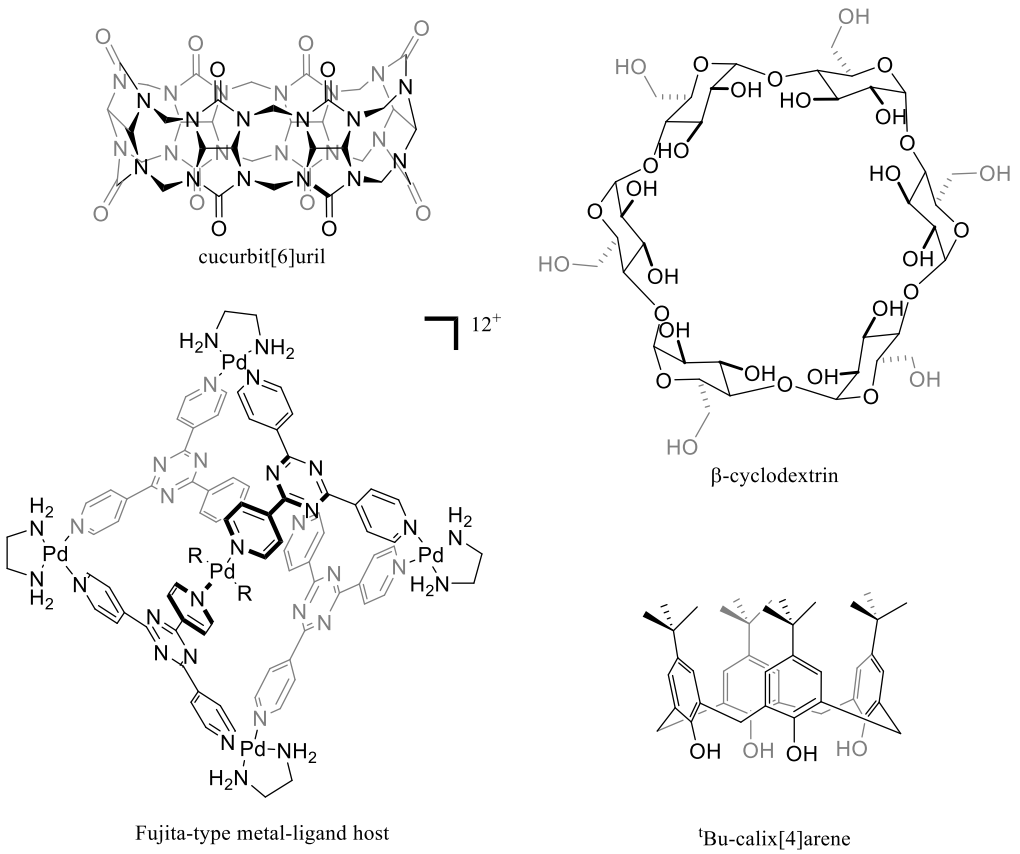

Figure 1. Cavity-containing hosts that provide a microenvironment distinct from bulk solution.

Certain enzymes convert starch to cyclic oligosaccharides known as cyclodextrins. The resulting macrocycles are inexpensive and used in commercial products like Febreze® and powdered ethanol.[15] These hosts encapsulate a wide variety of neutral and charged guests, with high binding affinities. Like many other aqueous hosts, cyclodextrins may endow lipophilic small molecules with water solubility, increase guest stability and decrease volatility.[16–18] Cyclodextrins number among the most effective enzyme mimics known, with million-fold rate accelerations for noncatalytic ester hydrolysis reactions, making their continued development crucial to the field of enzyme mimetics.[4,19–21]

Due to their potentially labile nature, metal-ligand coordination bonds have been widely used to construct supramolecular hosts of diverse form and function.[22,23] Metal-ligand hosts may be highly charged, which influences the scope and magnitude of guest encapsulation. Using design principles learned from forming small hosts, strategies to make much larger cavities have been developed.[24] Combining metal-ligand coordination with dynamic imine formation

has enabled the formation of a diverse array of new hosts which change form and stoichiometry depending on experimental conditions.[25] Complex metal-ligand knot-containing architectures have generated recent interest.[26] Metal-ligand hosts have also been shown to be competent catalysts, with rate accelerations among the highest reported with noncovalent hosts.[27] Metal-ligand coordination provides a general strategy to design a diverse selection of microenvironments applicable toward molecular recognition and catalysis.

As part of the latter group of hosts, $K_{12}Ga_4L_6$ tetrahedra have been shown to encapsulate neutral and cationic guests. These hosts are soluble in polar media and exhibit association constants of up to 10^5 M^{-1} for encapsulated guests and 10^3 M^{-1} for external binding.[28] Encapsulated transition metal catalysts may exhibit enhanced turnover compared to catalysts in bulk solution.[29] To date, a handful of diverse chemical reactions have been shown to be catalyzed by encapsulation in these tetrahedra.[27,30–34] Catalytic rate enhancements of up to 10^6 have been measured with good turnover.[27,30,31,35] Fundamental studies of the mechanism of proton exchange and use of these tetrahedra to catalyze the cyclizations of terpene derivatives are the focus of this dissertation.

References

(1) Faulkner, D. J. *Nat. Prod. Rep.* **2001**, *18* (1), 1.
(2) Haefner, B. *Drug Discov. Today* **2003**, *8* (12), 536.
(3) Whitesides, G. M. *Angew. Chem. Int. Ed.* **2015**, *54* (11), 3196.
(4) Breslow, R.; Dong, S. D. *Chem. Rev.* **1998**, *98* (5), 1997.
(5) Yoshizawa, M.; Klosterman, J. K.; Fujita, M. *Angew. Chem. Int. Ed.* **2009**, *48* (19), 3418.
(6) Freeman, W. A.; Mock, W. L.; Shih, N. Y. *J. Am. Chem. Soc.* **1981**, *103* (24), 7367.
(7) Mock, W. L.; Irra, T. A.; Wepsiec, J. P.; Adhya, M. *J. Org. Chem.* **1989**, *54* (22), 5302.
(8) Mock, W. L.; Irra, T. A.; Wepsiec, J. P.; Manimaran, T. L. *J. Org. Chem.* **1983**, *48* (20), 3619.
(9) Kim, K.; Selvapalam, N.; Ko, Y. H.; Park, K. M.; Kim, D.; Kim, J. *Chem. Soc. Rev.* **2007**, *36* (2), 267.
(10) Day, A.; Arnold, A. P.; Blanch, R. J.; Snushall, B. *J. Org. Chem.* **2001**, *66* (24), 8094.
(11) Cao, L.; Šekutor, M.; Zavalij, P. Y.; Mlinarić-Majerski, K.; Glaser, R.; Isaacs, L. *Angew. Chem. Int. Ed.* **2014**, *53* (4), 988.
(12) Cram, D. J.; Tanner, M. E.; Thomas, R. *Angew. Chem. Int. Ed. Engl.* **1991**, *30* (8), 1024.
(13) Zhang, Q.; Tiefenbacher, K. *J. Am. Chem. Soc.* **2013**, *135* (43), 16213.
(14) Zhang, Q.; Tiefenbacher, K. *Nat. Chem.* **2015**, *7* (3), 197.
(15) W, M.; W, S. Alcohol-containing powder. US3795747 A, March 5, 1974.
(16) Del Valle, E. M. M. *Process Biochem.* **2004**, *39* (9), 1033.
(17) Szejtli, J.; Szente, L. *Eur. J. Pharm. Biopharm.* **2005**, *61* (3), 115.
(18) Szejtli, J. *Chem. Rev.* **1998**, *98* (5), 1743.
(19) Zhang, B.; Breslow, R. *J. Am. Chem. Soc.* **1997**, *119* (7), 1676.
(20) Breslow, R. *Acc. Chem. Res.* **1995**, *28* (3), 146.
(21) Yan, J.; Breslow, R. *Tetrahedron Lett.* **2000**, *41* (13), 2059.
(22) Zarra, S.; Wood, D. M.; Roberts, D. A.; Nitschke, J. R. *Chem Soc Rev* **2015**, *44* (2), 419.
(23) Holliday, B. J.; Mirkin, C. A. *Angew. Chem. Int. Ed.* **2001**, *40* (11), 2022.
(24) Sun, Q.-F.; Iwasa, J.; Ogawa, D.; Ishido, Y.; Sato, S.; Ozeki, T.; Sei, Y.; Yamaguchi, K.; Fujita, M. *Science* **2010**, *328* (5982), 1144.

(25) Wood, D. M.; Meng, W.; Ronson, T. K.; Stefankiewicz, A. R.; Sanders, J. K. M.; Nitschke, J. R. *Angew. Chem. Int. Ed.* **2015**, *54* (13), 3988.
(26) Leigh, D. A.; Pritchard, R. G.; Stephens, A. J. *Nat. Chem.* **2014**, *6* (11), 978.
(27) Hastings, C. J.; Pluth, M. D.; Bergman, R. G.; Raymond, K. N. *J. Am. Chem. Soc.* **2010**, *132* (20), 6938.
(28) Sgarlata, C.; Mugridge, J. S.; Pluth, M. D.; Tiedemann, B. E. F.; Zito, V.; Arena, G.; Raymond, K. N. *J. Am. Chem. Soc.* **2010**, *132* (3), 1005.
(29) Brown, C. J.; Miller, G. M.; Johnson, M. W.; Bergman, R. G.; Raymond, K. N. *J. Am. Chem. Soc.* **2011**, *133* (31), 11964.
(30) Fiedler, D.; van Halbeek, H.; Bergman, R. G.; Raymond, K. N. *J. Am. Chem. Soc.* **2006**, *128* (31), 10240.
(31) Pluth, M. D.; Bergman, R. G.; Raymond, K. N. *J. Am. Chem. Soc.* **2008**, *130* (34), 11423.
(32) Pluth, M. D.; Bergman, R. G.; Raymond, K. N. *J. Org. Chem.* **2009**, *74* (1), 58.
(33) Hart-Cooper, W. M.; Clary, K. N.; Toste, F. D.; Bergman, R. G.; Raymond, K. N. *J. Am. Chem. Soc.* **2012**, *134* (43), 17873.
(34) Zhao, C.; Sun, Q.-F.; Hart-Cooper, W. M.; DiPasquale, A. G.; Toste, F. D.; Bergman, R. G.; Raymond, K. N. *J. Am. Chem. Soc.* **2013**, *135* (50), 18802.
(35) Hart-Cooper, W.; Zhao, C.; Triano, R.; Yaghoubi, P.; Ozores, H. L.; Burford, K.; Toste, F. D.; Bergman, R. G.; Raymond, K. *Chem. Sci.* **2014**.

Chapter 2
Water Exclusion by an Artificial Terpene Synthase Mimic

Introduction

Terpene synthases are enzymes that generate over thousands of small-molecule natural products from simple precursors.[1] These enzymes catalyze cascading 1,5-diene cyclization reactions that proceed through carbenium ion intermediates.[2] Noncovalent interactions, such as cation−π stabilization and steric repulsion, dictate the conformations of intermediates and resulting product distributions.[3,4] Although terpene synthases can be highly selective, product distributions containing multiple species are common. Contingent on the nature of the enzyme's active site, these intermediates may undergo eventual deprotonation or nucleophilic capture (e.g., by water) to furnish the final products.[5-7] An example is the conversion of geranyl diphosphate to limonene and α-terpineol via the α-terpinyl cation, as illustrated in Scheme 1.

Scheme 1. Biosynthesis of Limonene and α-Terpineol from Geranyl Diphosphate[a]

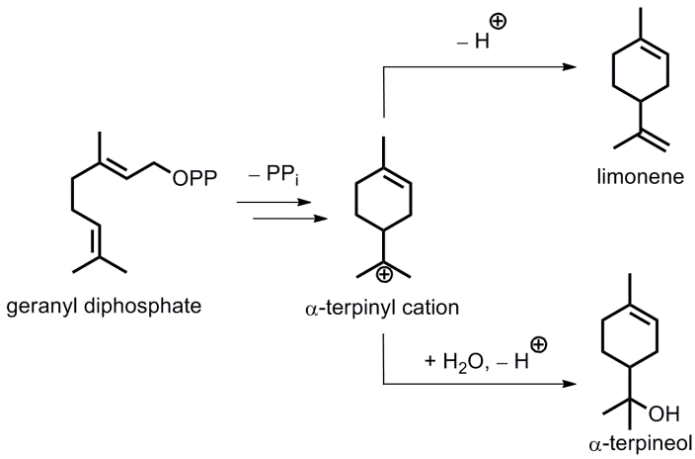

[a]PP_i = diphosphate. While limonene is obtained through a deprotonation route, capture of the α-terpinyl cation with water affords α-terpineol.[4-7]

Synthetic systems have modeled the selectivity and efficiency of enzymes.[8] Recent advances in supramolecular catalysis demonstrate the potential for these systems to effect high rate enhancements[9-11] and a capacity for regulation[12] reminiscent of enzyme catalysis. The Raymond group has developed a water-soluble, chiral metal–ligand assembly of $K_{12}Ga_4L_6$ stoichiometry (L = *N*,*N*-bis(2,3-dihydroxybenzoyl)-1,5-diaminonaphthalene; polyanion **1** represented in Scheme 2).[13] Bearing analogy to the active sites of terpene synthases,[14,7] the constrictive steric interior of polyanion **1** is defined by cation-stabilizing aromatic moieties. Combined with the assembly's high negative charge, this property has been demonstrated to bring about pK_a shifts for encapsulated guests.[15] Assembly **1** has consequently been shown to catalyze proton-mediated processes in basic solution.[16] Notably, **1** catalyzes the Nazarov cyclization of 1,3-pentadienols with rate accelerations on the order of 10^6 relative to background reactivity, which has been attributed to transition-state binding as well as substrate conjugate acid stabilization.[17]

Given the cation-stabilizing and hydrophobic properties of both the interior of **1** and the active sites of terpene synthases, the possibility of investigating a monoterpene cyclization in **1** was enticing. The monoterpene (±)-citronellal (**2**) has been shown to cyclize in the presence of Brønsted acids and is a relevant industrial intermediate in the manufacture of menthol.[18] It was hypothesized that **1**would stabilize the conjugate acid of encapsulated **2**, driving protonation at

the aldehyde oxygen and subsequent cyclization, the latter process being accelerated by the constrictive interior of **1**. Herein studies of a catalytic cyclization of **2** and two homologues (**6a**, **7a**) in a water-soluble supramolecular assembly at moderate temperatures and physiological pH is reported.

Scheme 2. Encapsulation of 2 by Host 1[a]

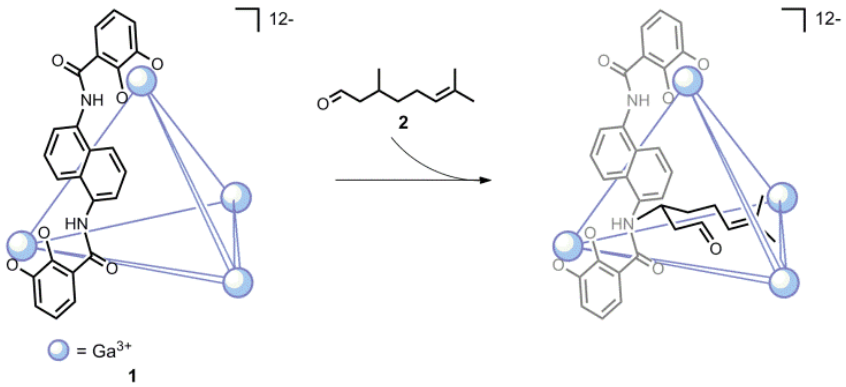

[a]Spheres represent a Ga^{3+} center, and bisbidentate ligands are depicted as lines.

Results and Discussion

It has been reported that three classes of products are formed when **2** is treated with acidic solution, as depicted in Scheme 3.[19-21] This was confirmed experimentally: in addition to minor products isopulegol (**3a**), neoisopulegol (**3b**), isoisopulegol (**3c**), and neoisoisopulegol (**3d**), a mixture of four stereoisomeric *p*-menthane-3,8-diols (**4**) is observed as the major class of products. Once formed, **4** may undergo condensation with **2** to generate *p*-menthane-3,8-diol citronellal acetal stereoisomers (**5**).[20] Compounds collectively designated **4** were observed to be composed of predominantly *cis* isomers (*cis*:*trans*, 3:2); minor components **3a**–**d** contained mostly *trans* products (*cis*:*trans*, 3:7). These distributions are consistent with a mechanistic divergence occurring at or before ring closing of **2**. Treating **3a**–**d** with a buffered solution of sufficient acidity to induce cyclization (pH 3.20, 60 °C, 2 h)[21] yielded a product mixture identical to that formed from the starting material, demonstrating that **3a**–**d** are persistent in an acidic aqueous environment at this pH and do not convert to corresponding *p*-menthane-3,8-diols. On the basis of these experiments, it is likely that the cyclization of **2** in acidic solution involves the two pathways leading to **3a**–**d** and **4** illustrated in Scheme 3.

Scheme 3. Proton-Mediated Cyclization of 2 to Products 3–5[a]

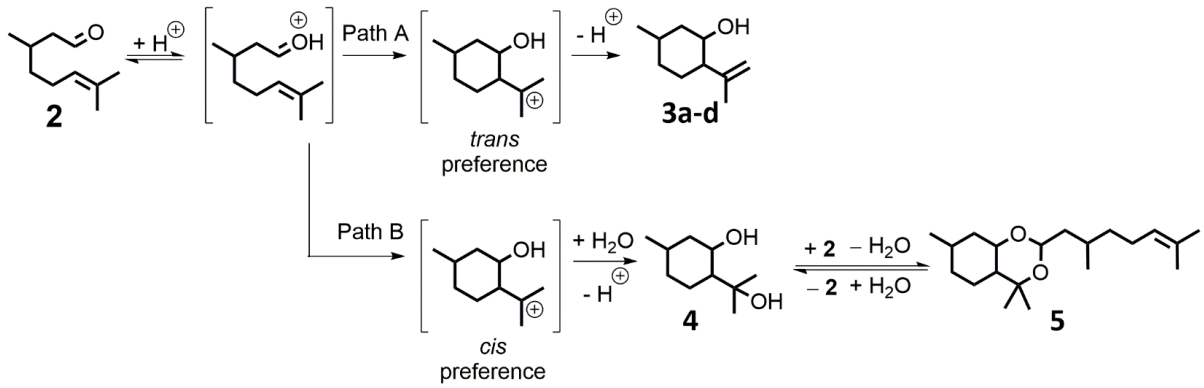

[a]Under catalysis by acidic solution, **3**–**5** are observed with **4** as the major product by Path B. Catalysis with **1** affords **3a**–**d** as the major class of products, demonstrating that Path A is instead favorable.

analysis of an aqueous mixture containing **2** and **1**, which exhibited a set of broad resonances shifted upfield by 1–3 ppm. Compound **2** was treated with an equivalent of **1** and the mixture heated for 18 h. Upon extraction and ^{1}H NMR analysis, the quantitative consumption of **2** was observed accompanied by new resonances corresponding to **3a**–**d**. Adding a slight excess of PEt_4^+, which is strongly encapsulated by **1**, halted this conversion. It was thus clear not only that the unblocked cavity of **1** was necessary for stoichiometric reactivity with **2**, but also that trace quantities of free ligand or Ga^{3+} could not be responsible for the observed transformation.[22] Treating **2** with 10 mol % of **1** resulted in the catalytic conversion of **2** to stereoisomeric products **3a**–**d** (Scheme 4). Due to the low solubility of **2**, the reaction mixture was heterogeneous and stirred vigorously. The ratio of *cis* to *trans* product did not differ appreciably from that observed for **3a**–**d** in acidic solution. Trace amounts of the stereoisomeric mixture **4** were also observed, the presence of which can be accounted for by background reactivity.[23] Isolated **4** did not undergo any transformation (e.g., dehydration) when treated with **1**. Thus, in contrast to cyclization in acidic solution, alkene products **3a**–**d** form with high selectivity upon treatment of **2** with **1** (Table 1).

Scheme 4. Selectivity of Alkene Products from the Cyclization of 2 by 1

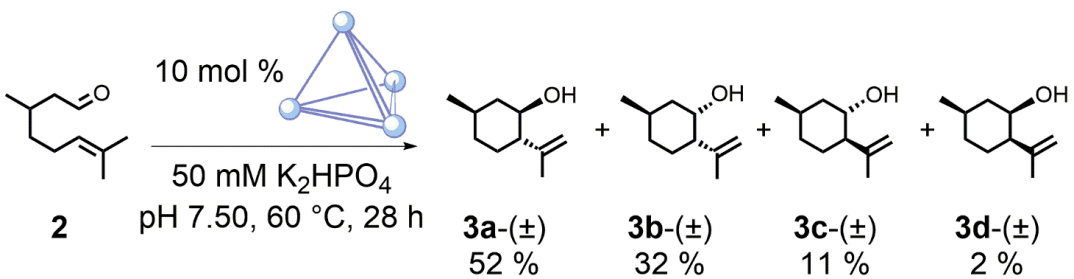

When incorporated in the backbone of acyclic substrates capable of undergoing cyclization, *gem*-dimethyl substitution has been shown to bring about increased cyclization rates (the *gem*-dimethyl effect) and, in some cases, product selectivity.[24] It has been hypothesized that this effect arises from conformationally destabilized ground states of *gem*-dimethyl-substituted

substrates compared to those lacking substitution.[25] Similarly, the efficiency of certain enzyme-catalyzed cyclizations has been attributed in part to conformational control of the bound substrate by the enzyme active site.[26] For example, limonene synthase is thought to bind intermediate linalyl diphosphate in a cisoid conformation, facilitating electrocyclization to an α-terpinyl cation.[7]

Table 1. The cyclization of 2 to 3-5 by 1 and buffered acidic solution

				Selectivity (%)		
Entry	Catalyst	pH	Conv. (%)	**3a-d**	**4**	**5**
1[a]	**1**	7.50	71	97	3	< 1[c]
2[b]	KH_2PO_4	3.20	91	9	91	< 1

Conversion and selectivity assessed by ^{1}H NMR. Selectivity determined as a proportion of the identified product. Aqueous solutions contained 50 mM phosphate buffer for both trials. Conditions: [a]10 mol % **1**, 60 °C, 28 h; [b]50 °C, 8 h; [c]Product not observed by ^{1}H NMR or GC-MS.

Given the conceptual similarity between the *gem*-dimethyl effect and certain instances of enzyme catalysis, the effect of *gem*-dimethyl substitution on product selectivity was examined. The structure of **2** was varied by replacing −Me and −H *β*-substituents with dihydro or dimethyl substitution, affording achiral homologues **6a** and **7a** (Scheme 5). The effect of these substitutions on product selectivity became apparent when **6a** and **7a** were treated with acidic solution. Like **2**, **6a** cyclized to predominantly stereoisomeric diols, **6d** and **6e**. However, in the absence of *gem*-dimethyl substitution, **7a** formed a complex mixture of products.[27] In contrast, when treated with **1**, both **6a** and **7a** cyclized to predominantly *trans*-alkene products (**6b** and **7b**, respectively), demonstrating that encapsulation in **1** affords conformational control during cyclization (Table 2).

Scheme 5. Proton-Mediated Cyclization of 6a and 7a to Products 6b−e and 7b−e

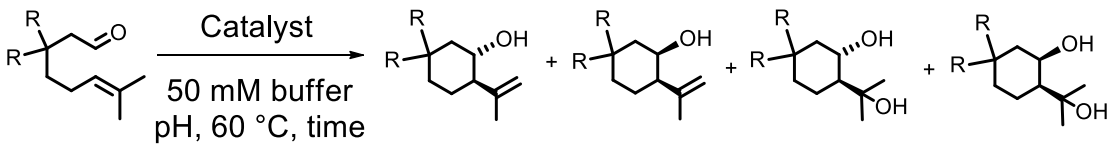

6a (R = Me) **7a** (R = H) **6b/7b**-(±) **6c/7c**-(±) **6d/7d**-(±) **6e/7e**-(±)

The *trans* product selectivity of **6a** in acidic solution is presumably the result of a 1,3-diaxial repulsion between the aldehyde oxygen and axially oriented β-methyl group in the transition state leading to *cis* product. The complex product mixture observed upon treating **7a** with acidic buffer demonstrates that in acidic solution, alternate reaction pathways are competitive with cyclization when *gem*-dimethyl substitution is absent at the β-position. In light of the very different product selectivity observed between **6a** and **7a** following acidic solution treatment, the tendency for these substrates to stereoselectively form alkene products in **1** is surprising, given that both bulk solution and cluster catalysis are proton-mediated processes. While the presence of *gem*-dimethyl substitution vastly improves the product selectivity obtained from

acidic solution catalysis, this discrepancy is eliminated with **1**. In the latter case, overriding steric repulsion experienced by the guest during encapsulation confers high selectivity toward *trans*-alkene products, regardless of whether *gem*-dimethyl substitution is present at the β-position.

Table 2. The cyclization of 6a and 7a by 1 and buffered acidic solution

				Selectivity (%)			
Substrate	Catalyst	pH	Conv. (%)	**6b/7b**	**6c/7c**	**6d/7d**	**6e/7e**
6a (R = Me)	**1** (10 mol %)	7.50	91	83	14	3	< 1[d]
6a (R = Me)	KH_2PO_4	3.20	80	3	< 1[d]	75	22
7a (R = H)	**1** (10 mol %)	7.50	60	87	11	< 1[d]	2
7a (R = H)	KH_2PO_4	3.20	> 95	nd[e]	nd[e]	nd[e]	nd[e]

Conversion and selectivity assessed by ^{1}H NMR. Selectivity determined as a proportion of the identified product. Aqueous solutions contained 50 mM phosphate buffer for all trials. Conditions: 60 °C; [a]28 h; [b]18 h; [c]20 h; [d]Product not observed by ^{1}H NMR or GC-MS; [e]Complex product mixture obtained—selectivity was not determined.

Having established enzyme-like selectivity in the Prins cyclizations of **2**, **6a**, and **7a**, it was then investigated whether **1** would impart similar selectivity during transition-metal-mediated transformations. Our group has recently reported the gold(I) host–guest complex $Me_3PAu^+\subset$**1** (where ⊂ denotes encapsulation) to be a viable catalyst for the hydroalkoxylation of allenes in water.[28] Gold-catalyzed cycloisomerizations of 1,6-enynes have been well documented to result in different products depending on reaction conditions and substituent effects.[29] In the absence of assembly **1**, Me_3PAuCl catalyzed the cycloisomerization of **8** to **10**, which was obtained in 85% yield (Scheme 6).[30] When the cavity of **1** was blocked by strongly bound NEt_4^+, compound **10** was likewise observed as the sole product. Use of Me_3PAuBr as a catalyst resulted in a lower yield of **10**, presumably due to a relatively strong gold–bromide bond and lower aqueous solvation of bromide compared to chloride. However, following treatment of **8** with $Me_3PAu^+\subset$**1**, **9** was instead produced as the major product. Preparing the encapsulation complex $Me_3PAu^+\subset$**1** from Me_3PAuBr instead of Me_3PAuCl did not have a significant effect on the selectivity of this process, and again 60:40 mixtures of products **9**:**10** resulted. The tendency for **1** to exclude water from reactive intermediates was thus demonstrated for a gold-catalyzed cycloisomerization of enyne **8**.

Scheme 6. Gold-Catalyzed Cycloisomerization of Enyne 8 to Products 9 and 10

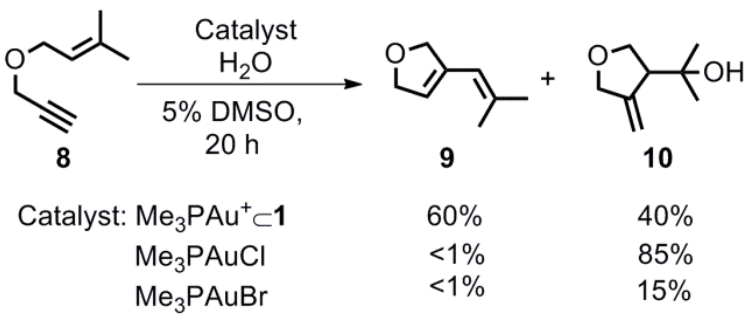

Conclusion

The first example of a terpene cyclization by a water-soluble supramolecular catalyst at physiological pH is reported. In analogy with the active sites of many terpene synthases, **1** directs the cyclization of monoterpene **2** toward deprotonation instead of nucleophilic capture by water.[31] The generality of this property was demonstrated in the gold-catalyzed cycloisomerization of enyne **8**. This effect can be attributed to the hydrophobic environment of the assembly's cavity, which prevents water from capturing carbenium ion intermediates during catalysis. Identification of **3a**–**d** is of interest, as these compounds are frequently used in the asymmetric synthesis of complex natural products.[32] The synthesis of **3a** from **2** is conventionally accomplished using organic solvents and Lewis acids, where dehydration and dimerization products are often observed.[33,34] In contrast, catalysis by **1** provides an environmentally benign method to afford products of synthetic and economic utility without the byproducts often observed from Lewis acid treatment.[35] Also, in contrast to cyclization in acidic solution, assembly **1** affords product selectivity in both the presence and the absence of *gem*-dimethyl substitution. This effect attests to the high degree of substrate conformational control provided by **1**. Both conformational control and the exclusion of water from reactive intermediates are characteristic properties of terpene synthases, to which the activity of **1** presented here bears analogy.

Experimental

General Experimental Procedures. Unless otherwise noted, reactions and manipulations were performed using standard Schlenk techniques or in an oxygen-free wet box under nitrogen atmosphere. Glassware was dried in an oven at 150 °C or by flame before use. Column chromatography was carried out on a Biotage SP1 MPLC instrument with prepacked silica gel columns.

Instrumentation. NMR spectra were obtained on a Bruker AV 400 (400 MHz), AV 500 (500 MHz) or AV 600 (600 MHz) spectrometer. Chemical shifts are reported as δ in parts per million (ppm) relative to residual protiated solvent resonances. NMR data are reported according to the format s = singlet, d = doublet, t = triplet, m = multiplet, b = broad; integration; coupling constant. Mass spectral data were obtained at the QB3 Mass Spectrometry Facility operated by the College of Chemistry, University of California, Berkeley. Electrospray ionization (ESI) mass spectra were recorded on a Finnigan LTQ FT mass spectrometer. GC-MS data were obtained on an Agilent Technologies 6890N/5973 GC-MS with HP-5MS column of 30 m length and 0.25 mm diameter. The separation method used an initial oven temperature of 40 °C (3 min), followed by a 10 °C/min ramp until 200 °C was reached, which was then followed by a 15 °C/min ramp until 300 °C was attained and this temperature held for 5 min.

Materials. Unless otherwise noted, chemicals were obtained from commercial suppliers and used without further purification. The synthesis of $K_{12}Ga_4L_6$ (K_{12}**1**) and **6a** has been described.[13,36] All solvents were degassed under nitrogen for 20 min before use.

Stoichiometric treatment of 2 with 1. Two reaction mixtures were prepared by adding K_{12}**1** (15 mg, 4.2 μmol) in 500 μL D_2O to an NMR tube. Both tubes were capped with rubber septa. To the first reaction mixture, PEt_4Br (6.2 μmol, 1.4 mg) was added, followed by **2** (4.0 μmol, 0.62 mg). The second reaction mixture was prepared in an identical manner except that no PEt_4Br was added. Both reaction mixtures were heated to 50 °C in an oil bath for 18 h, after which the organic portion was extracted (3 x 200 μL $CDCl_3$) and analyzed by ^{1}H NMR. While the organic extract from the first reaction mixture afforded a ^{1}H NMR spectrum identical to

that of the starting material **2**, the extract from the unblocked trial exhibited quantitative (> 95%) conversion of **2** to **3a-d**. Treating a solution of K_{12}**1** (15 mg, 4.2 μmol in 400 μL D_2O) with an excess of **2** (40 μmol, 6.2 mg), followed by ^{1}H NMR analysis, permitted the observation of broad upfield resonances characteristic of encapsulation.

General Procedure for the Catalytic Cyclization of 2, 6a and 7a by 1. Aldehyde **2**, **6a** or **7a** (44 μmol), K_{12}**1** (4.2 μmol, 15.0 mg) and 400 μL phosphate buffer (50 mM K_2HPO_4, pH 7.50) were added to a one dram vial equipped with magnetic stir bar. This heterogenous mixture was stirred vigorously and heated in an oil bath at 60 °C for 28 h, after which the organic products were extracted (3 x 300 μL $CDCl_3$) and passed through a pipet containing a thin filter of glass fiber. Compounds **3a-d,**[33b,37] **4**[38] (two major stereoisomers), **6b-e**[33a,39] and **7b-e**[40,41] were identified by matching their ^{1}H and ^{13}C{^{1}H} NMR resonances, MS fragmentation patterns and relative GC retention times to literature data. Integration of the unique alcohol C-*H* resonances in the crude organic mixture was used to determine product distribution. Yield and conversion were assessed against an internal standard of *o*-xylene. Product selectivity is reported as a proportion of identified product. Treating **2** with **1** resulted in 71% conversion of **2** to products **3a-d,** which were obtained in 65% total yield (product selectivity: 52% **3a**, 32% **3b**, 11% **3c**, 2% **3d**, 3% **4**, < 1% **5**; **5** was not observed by ^{1}H NMR or GC-MS. Treating **6a** with **1** resulted in 91% conversion of **6a** to products **6b-e,** which were obtained in 87% total yield (product selectivity: 83% **6b**, 14% **6c**, 3% **6d** and < 1% **6e**). Treating **7a** with **1** resulted in 60% conversion of **7a** to products **7b-e**, which were obtained in 55 % total yield (product selectivity: 87% **7b**, 11% **7c**, < 1% **7d** and 2% **7e**). Under conditions identical to those described above, treating **4** (44 μmol, 3:2, *cis*:*trans*) with **1** (4.2 μmol) resulted in no further transformations (as determined by ^{1}H NMR), thereby eliminating the possibility that **1** dehydrates **4** to **3a-d** under the reaction conditions employed. In the absence of **1**, subjecting **2** to the above conditions led to low (4%) yield of **4**, demonstrating that the low proportions of diol products observed in the previous trials can be accounted for by background reactivity. Likewise, treating **2** (44 μmol) with an excess of neutral ligand (10 mg, 23 μmol) or $Ga(acac)_3$ (10 mg, 27 μmol) under the above conditions resulted in recovery of **2**, 4% yield of **4** and neither **3** nor **5** observed by ^{1}H NMR. After treatment with $Ga(acac)_3$, a small amount (~10%) of unidentified side products was observed.

General Procedure for the Cyclization of 2, 6a and 7a in Acidic Buffer Solution. Aldehyde **2**, **6a** or **a** (44 μmol) and 400 μL phosphate buffer (50 mM KH_2PO_4, pH 3.20) were added to a one dram vial equipped with a magnetic stir bar. This heterogenous mixture was stirred vigorously and heated in an oil bath. Compound **2** was heated at 50 °C for 8 h, while **6a** and **7a** were heated at 60 °C for 20 h and 18 h, respectively. The organic products were then extracted (3 x 300 μL $CDCl_3$) and passed through a pipet containing a thin filter of glass fiber. The two major stereoisomers represented by structure **5** were identified by ^{1}H NMR resonances, MS fragmentation patterns and relative GC retention times.[38] Integration of the unique alkene C-*H* (for **2**, **3a-d**) alcohol C-*H* (for **4**, **6d**/**7d** and **6e**/**7e**) and acetal C-*H* (for **5**) resonances in the crude organic mixture was used to determine product distribution. Yield and conversion were assessed against an internal standard of *o*-xylene. Product selectivity is reported as a proportion of identified product. Treating **2** with acidic buffer resulted in 91% conversion of **2** to products **3a-d,** which were obtained in 80% total yield (product selectivity: 9% **3a**-d, 91% **4** and < 1% **5**). In contrast to the **1**-catalyzed cyclization of **2**, trace quantities of **5** were present. Treating **6a** with acidic buffer likewise resulted in 91 % conversion of **6a** to products **6b**, **6d** and **6e** which were obtained in 86% total yield (product selectivity: 3% **6b**, <

1% **6c**, 75% **6d** and 22% **6e**; compound **6c** was not observed by ^{1}H NMR or GC-MS). Treating **7a** with acidic buffer resulted in > 95% conversion of **7a** to an intractable mixture of products. In addition to the products which were soluble in $CDCl_3$, an insoluble white precipitate was present, presumably a polymer formed from an acid-catalyzed aldol condensation of **7a**. Further product characterization was consequently not pursued with the latter mixture.

Assessing Alkene Hydration of 3a-d in Acidic Buffer Solution. A commercial mixture of **3a-d** (1 mmol, 154 mg, stereoisomer proportions determined by ^{1}H NMR: 65 % **3a**, 28% **3b**, 6% **3c**, 2% **3d**) and 5.00 mL of acidic buffer solution (50 mM phosphate buffer, pH 3.20) was added to a 25 mL round-bottom flask with a magnetic stir bar. The mixture was heated and stirred for 2 h at 60 °C. The organic portion was then extracted (3 x 5 mL DCM), dried over $MgSO_4$, filtered and concentrated under vacuum to yield the crude product, which was analyzed by GC-MS. The GC trace and corresponding mass spectra were identical to those of the starting material. In contrast, when **2** was substituted for **3a-d** under otherwise identical conditions, low levels of conversion (46%) to **3a-d**, **4** and **5** were observed, a quantity which is in agreement with a previously reported account.[21]

Preparation of 7a. To a 10 mL vial charged with magnetic stir bar, second generation Grubbs catalyst (8.2 mg, 0.0097 mmol), 2-methyl-2-butene (2.100 g, 30.00 mmol) and **8** (130 mg, 0.93 mmol) were added. The red reaction mixture was stirred lightly at room temperature (23 °C) for 31 h. The mixture was treated with DMSO (1.65 mg, 21 mmol) for 19 hours as a homogenous solution, followed by silica gel chromatography (1 – 20 % EtOAc in hexanes gradient over 10 column volumes) to remove ruthenium byproducts,[42] affording compound **7a**[43] as a colorless oily liquid in 83% (108 mg, 0.77 mmol) yield. This yield excludes residual **8**, which was present as a 4% molar impurity.

Preparation of 6d and 6e. 6a (130 mg, 0.77 mmol) was treated with acidic buffer (5.00 mL, 50 mM KH_2PO_4, pH 3.20) in a 10 mL vial charged with a magnetic stir bar. This heterogenous mixture was stirred at 60 °C for 24 h, after which the organic portions were extracted with DCM (3 x 5 mL). DCM was removed under vacuum and the resulting crude oily liquid passed through a silica gel column (10–35% EtOAc in hexanes gradient over 10 column volumes) to yield isolated **6d** (34 mg, 0.20 mmol, 26%) and **6e** (10 mg, 0.06 mmol, 8%) as colorless crystalline solids. Low isolated yields were obtained due to poor separation of **6d** from **6e**.

6d: ^{1}H NMR (600 MHz, $CDCl_3$): δ 3.95 (dt, 1H, J = 10.2, 4.1 Hz), 3.40 (br s, 1H), 1.72 (m, 1H), 1.61 (m, 2H), 1.39 (m, 2H), 1.27 (s, 3H), 1.22 (s, 3H), 1.16-1.21 (m, 2H), 1.11-1.14 (m, 1H), 1.03 (s, 3H), 0.94 (s, 3H). $^{13}C\{^1H\}$NMR δ 23.7, 23.8, 24.9, 30.1, 32.2, 32.7, 38.8, 48.8, 54.2, 69.9, 75.0; HRMS-ESI (*m*/*z*): Exact mass calcd for $C_{11}H_{23}O_2$ $[M]^+$: 187.1693, found 187.1696.

6e: ^{1}H NMR (600 MHz, $CDCl_3$): δ 4.41 (br s, 1H), 1.89-1.78 (m, 1H), 1.68-1.55 (s, 3H), 1.32 (s, 3H), 1.26-1.31 (m, 2H), 1.25 (s, 3H), 1.24-1.15 (m, 2H), 1.12 (s, 3H), 1.10-0.98 (m, 1H), 0.88 (s, 3H). $^{13}C\{^1H\}$NMR δ 17.1, 27.2, 28.7, 28.8, 29.4, 33.9, 39.7, 46.2, 48.8, 69.1, 73.1. HRMS-ESI (*m*/*z*): Exact mass calcd for $C_{11}H_{23}O_2$ $[M]^+$: 187.1693, found 187.1697.

Preparation of 3-Methyl-1-(prop-2-ynyloxy)but-2-ene 8: Propargyl bromide (3.82 mL, 25.7 mmol, 80% solution in toluene) was added dropwise to a stirred solution of 3-methyl-2-buten-1-ol (2.00 mL, 19.8 mmol), tetrabutylammonium hydrogensulfate (327 mg, 0.990 mmol), and sodium hydroxide (3.17 g, 79.2 mmol) in water (1.5 mL). The reaction mixture was stirred for 20 hours at room temperature. The solid was removed by filtration and washed with diethyl ether. The filtrate was poured into water and extracted three times with diethyl ether. The combined organic fractions were washed with brine, dried with magnesium sulfate, and

concentrated. Flash chromatography on silica gel (4% Et_2O in pentanes eluant) afforded the purified product **8** as a colorless liquid (2.18 g, 17.5 mmol, 89% yield). ^{1}H NMR chemical shifts corresponded with those reported in the literature.[44]

Cyclization of 8 with $Me_3PAu^+ \subset$**1**: The enyne **8** (8.0 mg, 0.064 mmol) and the internal standard 1,3,5-trimethoxybenzene (3.6 mg, 0.022 mmol) were weighed into a 1 dram vial and capped with a teflon/silicon septum cap. The vial was purged with nitrogen for fifteen minutes and sealed with parafilm paper. Meanwhile, chloro(trimethylphosphine) gold (2.0 mg, 0.0064 mmol) was weighed into a separate vial. Both vials were then brought into a glovebox. The cluster K_{12}**1** (28 mg, 0.0077 mmol) was weighed into the vial containing the gold catalyst and water (2.0 mL) was added. The resulting solution was stirred for twenty minutes. DMSO (100 µL) was added to the vial containing the enyne **8** and the internal standard. The solution of $Me_3PAu^+ \subset$**1** was then filtered through a microsyringe filter tip into the vial containing **8**, which was then capped, removed from the glovebox, and sealed with parafilm paper. After 20 hours of stirring at room temperature the product was extracted with $CDCl_3$ (1 mL) and dried by passing through a pipette filled with magnesium sulfate, directly into an NMR tube for analysis. The yield (60% **9**, 40% **10**) was determined relative to the internal standard. This procedure was repeated with Me_3PAuBr used to generate $Me_3PAu^+ \subset$**1** rather than Me_3PAuCl, and gave the same result. Under otherwise identical conditions to those described above, addition of NEt_4Cl (1.6 mg, 0.0096 mmol) resulted in formation of only **10** in 57 % yield. The diene product **9** was not detected by ^{1}H NMR. The peaks corresponding to **9** and **10** were assigned by comparison with an authentic sample of **9** (prepared by Me_3PAuCl mediated cycloisomerization under anhydrous conditions) or literature reported chemical shift values of **10**.[44]

Cyclization of 8 with Me_3PAuCl**:** The enyne **8** (8.0 mg, 0.064 mmol), internal standard 1,3,5-trimethoxybenzene (10.8 mg, 0.0644 mmol), and chloro(trimethylphosphine) gold (2.0 mg, 0.0064 mmol) were weighed into a one dram vial. Water (2.0 mL) and DMSO (100 µL) were added and the vial capped. The mixture was stirred at room temperature for twenty hours at which time the product was extracted with $CDCl_3$ (1 mL), and dried by passing through a pipette filled with magnesium sulfate directly into an NMR tube for analysis. An analogous procedure was adopted for the cyclization of **8** with Me_3PAuBr.

Preparation of 9 for characterization purposes: Chloro(trimethylphosphine)gold (10 mg, 0.032 mmol) and silver hexafluoroantimonate (11 mg, 0.033 mmol) were weighed into a dry round bottom flask that was then purged with nitrogen. Dry dichloromethane (5 mL) was then added and the flask was cooled to -78 °C in a dry ice/isopropanol bath. The enyne **8** (200 mg, 1.61 mmol) was added dropwise by microliter syringe. The reaction mixture was stirred at this temperature for thirty minutes and was then warmed to room temperature. The solution was filtered through Celite and concentrated. Flash chromatography on silica gel (4% Et_2O in pentanes eluant) afforded 174 mg (1.41 mmol, 87% yield) of the purified product 3-methylene-4-(propan-2-ylidene)tetrahydrofuran **9** as a colorless liquid. ^{1}H NMR (400 MHz, $CDCl_3$) δ 6.58 (d, *J* = 10.4 Hz, 1H), 5.79 (d, *J* = 10.3 Hz, 1H), 4.40 (s, 2H), 4.24 (s, 2H), 1.82 (s, 3H), 1.74 (s, 3H); ^{13}C NMR (100 MHz, $CDCl_3$) δ 127.1, 124.7, 124.4, 123.2, 66.0, 65.5, 19.7, 19.4 mass spectrum (*m/z*) 124 (75, M+), 81 (100); HRMS calc'd for $C_8H_{12}O$: 124.0888; found: 124.0890.

References

1. Köksal, M.; Hu, H.; Coates, R. M.; Peters, R. J.; Christianson, D. W. *Nat. Chem. Biol.* **2011**,7, 431

2. Christianson, D. W. *Chem. Rev.* **2006**, 106, 3412
3. Faraldos, J. A.; Antonczak, A. K.; González, V.; Fullerton, R.; Tippmann, E. M.; Allemann, R. K. *J. Am. Chem. Soc.* **2011**, 133, 13906
4. Degenhardt, J.; Köllner, T. G.; Gershenzon, J. *Phytochemistry* **2009**, 70, 1621
5. Wheeler, C. J.; Croteau, R. *J. Biol. Chem.* **1987**, 17, 8213
6. Martin, D. M.; Bohlmann, J. *Phytochemistry* **2004**, 65, 1223
7. Hyatt, D. C.; Youn, B.; Zhao, Y.; Santhamma, B.; Coates, R. M.; Croteau, R. B.; Kang, C.*Proc. Natl. Acad. Sci. U.S.A.* **2007**, 104, 5360
8. For reviews, see:
   (a) Avram, L.; Cohen, Y.; Rebek, J., Jr. *Chem. Commun.* **2011**, 47,5368
   (b) Purse, B. W.; Rebek, J., Jr. *Proc. Natl. Acad. Sci. U.S.A.* **2005**, 102, 10777
   (c) Yoshizawa, M.; Klosterman, J. K.; Fujita, M. *Angew. Chem., Int. Ed.* **2009**, 48, 3418
   (d) Breiner, B.; Clegg, J. K.; Nitschke, J. R. *Chem. Sci* **2011**, 2, 51
   (e) Weister, M. J.; Ulmann, P. A.; Mirkin, C. A. *Angew. Chem., Int. Ed.* **2010**, 50, 114
   (f) Meeuwissen, J.; Reek, J. N. H. *Nat. Chem* **2010**, 2, 615 and references therein
9. Hastings, C. J.; Pluth, M. D.; Bergman, R. G.; Raymond, K. N. *J. Am. Chem. Soc.* **2010**, 132,6938
10. Mock, W. L.; Irra, T. A.; James P. Wepsiec, J. P.; Adhya, M. *J. Org. Chem.* **1989**, 54,5302
11. Marinescu, L. G.; Bols, M. *Angew. Chem., Int. Ed.* **2006**, 45, 4590
12. Yoon, H. J.; Kuwabara, J.; Kim, J.-H.; Mirkin, C. A. *Science* **2010**, 330, 66
13. Caulder, D. L.; Powers, R. E.; Parac, T. N.; Raymond, K. N. *Angew. Chem., Int. Ed.* **1998**,37, 1840
14. Reinert, D. J.; Balliano, G.; Schulz, G. E. *Chem. Biol.* **2004**, 11, 121
15. Pluth, M. D.; Bergman, R. G.; Raymond, K. N. *J. Am. Chem. Soc.* **2007**, 129, 11459
16. Pluth, M. D.; Bergman, R. G.; Raymond, K. N. *Acc. Chem. Res.* **2009**, 42, 1650 and references therein
17. (a) Hastings, C. J.; Pluth, M. D.; Bergman, R. G.; Raymond, K. N. *J. Am. Chem. Soc.* **2010**,132, 6938
    (b) Hastings, C. J.; Backlund, M. P.; Bergman,R. G.; Raymond, K. N. *Angew. Chem., Int. Ed.* **2011**, 50, 1
18. Lenardao, E. J.; Botteselle, G. V.; de Azambuja, F.; Perin, G.; Jacob, R. G. *Tetrahedron***2007**, 63, 6671
19. Clark, B. C., Jr.; Chamblee, T. S.; Iacobucci, G. A. *J. Org. Chem.* **1984**, 49, 4557
20. Yuasa, Y.; Tsuruta, H.; Yuasa, Y. *Org. Process Res. Dev.* **2000**, 4, 159
21. Cheng, H.; Meng, X; Liu, R.; Hao, Y.; Yu, Y.; Cai, S.; Zhao, F. *Green Chem.* **2009**, 11,1227
22. Treating **2** with excess ligand or Ga^{3+} also did not afford **3a–d**; see experimental section for details.
23. Conditions in the absence of **1**: 28 h, 60 °C, pH 7.50; only 4% yield of **4** was observed as product from **2**; see experimental section for details.
24. Jung, M. E.; Piizzi, G. *Chem. Rev.* **2005**, 105, 1735 and references therein
25. Jung, M. E. *Synlett* **1990**, 4, 186– 190
26. (a) Page, M. J.; Jencks, W. P. *Proc. Natl. Acad. Sci. U.S.A.* **1971**, 68, 1678
    (b) Bruice, T. C.; Pandit, U. K. *Proc. Natl. Acad. Sci. U.S.A.* **1960**, 46, 402
27. An insoluble white precipitate formed over the course of 18 h; see experimental section for details.

28. Wang, Z. J.; Brown, C. J.; Bergman, R. G.; Raymond, K. N.; Toste, F. D. *J. Am. Chem. Soc*.**2011**, 133, 7358
29. For reviews see:
(a) Watson, I. D. G.; Toste, F. D. *Chem. Sci* **2012**, 3, 2899
(b) Núñez-Jiménez, E.; Echavarren, A. M. *Chem. Rev.* **2008**, 108, 3326
(c) Michelet, V.; Toullec, P. Y.; Genêt, J. P. *Angew. Chem., Int. Ed.* **2008**, 47, 4268
(d) Gorin, D. J.; Toste, F. D. *Nature* **2007**, 446, 395
(e) Zhang, L.; Sun, J.; Kozmin, S. A. *Adv. Synth. Catal.* **2006**, 348, 2271
30. As described in the experimental section, **10** has previously been observed under aqueous conditions (catalyst = $Hg(OTf)_2$), while **9** is observed when water is absent (catalyst = $AgSbF_6$).
31. For examples of dehydration reactions driven by supramolecular hosts, see:
Murase, T.; Nishijima, Y.; Fujita, M. J. *Am. Chem. Soc* **2012**, 134, 162 and references17a and 17b.
32. (a) Ferraz, H. M. C.; Grazini, M. V. A.; Ribeiro, C. M. R.; Brocksom, U.; Brocksom, T. J. *J. Org. Chem.* **2000**, 65, 2606
(b) Gill, S.; Kocienski, P.; Kohler, A.; Pontiroli, A.; Qun, L. *Chem. Commun.* **1996**, 1743
33. (a) Negoi, A.; Wuttke, S.; Kemnitz, E.; Macovei, D.; Parvulescu, V. I.; Teodorescu, C. M.; Coman, S. M. *Angew. Chem., Int. Ed.* **2010**, 49, 8134
(b) Silva, K. A.; Robles-Dutenhefner, P. A.; Sousa, E. M. B.; Kozhevnikova, E. F.; Kozhevnikov, I. V.; Gusevskaya, E. V. *Catal. Commun.* **2004**, 5, 425
34. No dimerization or dehydration products were observed (by ^{1}H NMR, GC-MS) from treatment of **2** with **1**.
35. For an alternative approach to controlling the outcome of terpene cyclization reactions, see:
Pronin, V. S.; Shenvi, R. A. *Nat. Chem.* **2012**, 1458.
36. Jeong, K. S.; Go, Y. B.; Shin, S. M.; Lee, S. J.; Kim, J.; Yaghi, O. M.; Jeong, N. *Chem. Sci*. **2011**, *2*, 877.
37. Characterization of **3a**-**d**: (a) Schulte-Elte, K. H.; Ohloff, G. *Helv. Chim. Acta*, **1967**, *50*, 153. (b) Castilho, P.; Liu, K.; Rodrigues, A. I.; Feio, S.; Tomi, F.; Casanova, J. *Flavour Fragr. J*. **2007**, *22*, 139.
38. Compound classes **4** and **5** each represent two major stereoisomers, as reported by Yuasa and coworkers: Yuasa, Y.; Tsuruta, H.; Yuasa, Y. *Org. Process Res. Dev.* **2000**, *4*, 159.
39. Characterization of **6c**: Funakoshi, K.; Togo, N.; Koga, I.; Sakai, K. *Chem. Pharm Bull*. **1989**, *37*, 1990.
40. Characterization of **7b**, **7c**: Mikama, K.; Terada, M.; Sawa, E.; Nakai, T. *Tetrahedron Lett.* **1991**, 6571; reference 33a.
41. Characterization of **7d**, **7e**: Foubelo, F.; Gutierrez, A.; Yus, M. *Synthesis* **1999**, 503. Maffrand, J. P.; Maroni, P. *Tetrahedron Lett.* **1969**, 4201.
42. Ahn, Y.; Yang, K.; Georg, G. *Org. Lett*. **2001**, *3*, 1411.
43. Characterization of **7a**: Sakane, S.; Maruoka, K.; Yamamoto, H. *Tetrahedron* **1986**, *42*, 2203.
44. Nishizawa, M.; Yadav, V. K.; Skwarczynski, M.; Takao, H.; Imagawa, H.; Sugihara, T. *Org. Lett*. **2003**, *5*, 1609.
45. This chapter was adapted from Hart-Cooper, W. M.; Clary, K. N.; Toste, F. D.; Bergman, R. G.; Raymond, K. N. *J. Am. Chem. Soc.* **2012**, *134*, 17873.

Chapter 3

Influence of Microenvironment on the Catalytic Cyclization of Terpene Derivatives

Introduction

Enzymes use precisely tailored binding pockets to mediate stereoselective catalysis.[1–5] For example, terpene synthases catalyze the cyclization of simple precursors to over 70,000 known small molecule natural products.[6–8] While these enzymes clearly demonstrate a high degree of chemical divergence, precisely how they do so is an area of continuing and fruitful investigation.

In recent years, the field of supramolecular catalysis has progressed toward understanding the role of chemical microenvironments during catalysis.[9–23] Analogous to the active sites of many enzymes, synthetic hosts mediate catalysis through the organization of catalytically relevant functional groups that lower activation barriers relative to those that would be present in bulk solution. These strategies have relied on local concentration effects, electrostatics, pK_a shifts and the use of host-guest orientation to stabilize high-energy intermediates and transition states.

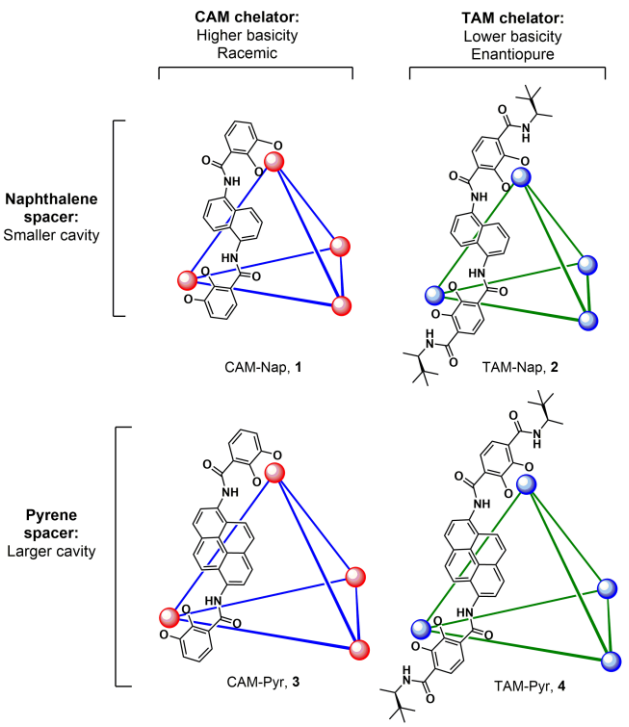

Figure 1. $K_{12}Ga_4L_6$ assemblies discussed in this work. Spheres represent Ga^{3+} centers and lines represent ligands as depicted (CAM = catecholamide, TAM = terephthalamide, Nap = naphthalene, Pyr = pyrene). Only one ligand enantiomer is shown for **2** and **4**. Potassium ions are omitted for clarity.

Our group has previously reported the use of a racemic, homochiral (Λ_4 or Δ_4) $K_{12}Ga_4L_6$ tetrahedron ((±)-**1**) to catalyze the Prins cyclization of monoterpene derivatives.[24] While catalytic antibodies[25–28] have been shown to mimic key properties of terpene synthases, the tetrahedron described above acts as a purely synthetic active site mimic.[29] In contrast to catalysis in acidic aqueous solution, which affords cyclic diol products, host-catalyzed

cyclizations resulted in high selectivity for alkene products. This example of selectivity parallels that of terpene synthases such as limonene synthase.[30] In a more recent development, a chiral ligand that self-assembles in an enantiopure fashion was prepared, affording enantiomeric terephthalamide-based hosts (Λ_4- or Δ_4-**2**, Figure 1). These hosts were observed to catalyze an enantioselective variant of the Prins reaction.[31] Inhibition experiments have indicated that catalysis proceeds initially through substrate encapsulation, which is reversible and rapid.[24,32,33] In light of these developments, investigation into the sources of the observed chemo-, diastereo-, and enantioselectivities of these reactions was pursued.

A mechanistic study is presented of the Prins cyclization in supramolecular host catalysts whose structures were systematically varied in the choice of chelator (CAM = catecholamide, TAM = terephthalamide) and spacer (Nap = naphthalene, Pyr = pyrene). Differences in catalytic rate, as well as product chemo-, diastereo- and enantioselectivity were found. The nature of host-mediated enantioinduction was investigated through the kinetic resolution of racemic substrates. These studies are supported by kinetic analysis and quantitative rate accelerations that provide an improved understanding of host structure on a chemoselective and stereochemically complex reaction.

Results and discussion

Effects of host structure on product selectivity. Differences in selectivity were examined by varying the structures of both hosts and substrates. It has been established that host catalysts often exhibit strict substrate selectivity based on guest size.[34,35] Following this precedent, the interaction of host and substrate size was tested by examining the effect of increasing host cavity volume on reaction stereoselectivity. Earlier reports have documented the difficulty of preparing pyrene-core host (±)-**3** in the absence of a strongly-bound template.[36] However, treatment of reaction mixtures containing appropriate metal and ligand components with KOH and acetone allowed for the isolation of (±)-**3** and **4**, in analogy with the procedure reported for the preparation of solvent-occupied (±)-**1**.[37] Previously, Δ_4-**1** mediated enantioselectivities of up to 78% in the aza-Cope rearrangement of enammonium cations and 69% in intramolecular Prins reactions were observed, a result which attests to the potentially high degree of enantiodifferentiation between Δ_4-**1** and catalytically relevant substrates.[31,38] These examples of molecular recognition have been attributed to predominantly steric and π-interactions, as chiral induction is thought to proceed through contact of guest with naphthalene spacers. Given this precedent, the investigations reported herein were focused on a class of substrates that differ in their alkyl substituents at the β-position but are otherwise identical with regard to functional groups. This modification was aimed at avoiding the introduction of additional functional groups[39–41] in the substrate that could dramatically alter the mechanism or stability of these compounds. Toward this end, terpene derivatives **5a-c** were separately treated with catalysts in either pure phosphate buffer solution or MeOD-d_4/100 mM phosphate buffer cosolvent. After heating, the organic portions of the reaction mixtures were extracted and product distributions measured by ^{1}H NMR integration. During these trials, product ratios were found to be insensitive to moderate changes in cosolvent composition, temperature, time and pD.

Initially, differences in product selectivity resulting from the choice of host chelator were examined by comparing product mixtures following treatment of various substrates with (±)-**1** and **2** (Scheme 1). The extent to which enantiopure **2** distinguishes between enantiomers (*S*)-**5a** and (*R*)-**5a** was tested. Note that this experiment is not possible with resolved (±)-**1** due to the presence of residual NMe_4^+, which inhibits catalysis.[31,42,43] Product ratios varied between

(a) Treatment of hosts **1-4** with chiral substrates **5a-c**

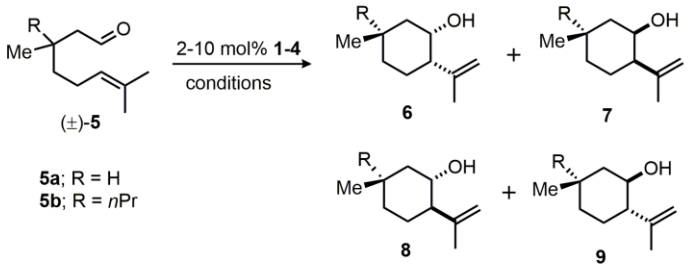

entry	host	substrate	mol%	temp/°C	time/h	%conv.	% **6**	% **7**	% **8**	% **9**
1a[a]	(±)-**1**	(±)-**5a**	10	60	28	71	33	2	11	54
2a[b]	Δ_4-**2**	(*S*)-**5a**	10	40	23	70	51	1	9	39
3a[b]	Δ_4-**2**	(*R*)-**5a**	5	40	23	60	30	1	8	61
4a[c]	(±)-**3**	(±)-**5a**	2	60	48	45	24	<1	4	71
5a[c]	Λ_4-**4**	(±)-**5a**	2	60	48	68	20	<1	30	50
6a[c]	Δ_4-**4**	(*S*)-**5a**	5	60	48	56	8	<1	34	58
7a[c]	Δ_4-**4**	(*R*)-**5a**	5	60	48	80	12	<1	30	58
8a[c]	(±)-**1**	(±)-**5b**	10	50	30	20	<1[e]	<1[e]	>95[f]	
9a[d]	Λ_4-**2**	(±)-**5b**	2	40	24	60	<1[e]	<1[e]	>95[f]	

(b) Treatment of hosts **1**, **2**, **4** with achiral substrate **5c**

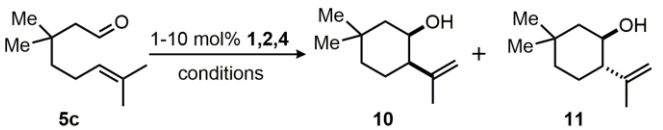

entry	host	mol%	temp/°C	time/h	%conv.	% **10**	% **11**	%ee of **11**
1b[a]	(±)-**1**	10	60	28	91	14	86	–
2b[c]	Δ_4-**2**	2.5	25	50	92	12	88	61
3b[c]	Δ_4-**2**	1	40	16	22	11	89	–
4b[c]	Λ_4-**4**	2	40	16	93	2	98	–33

Scheme 1. General conditions effective in the cyclizations of (a) chiral substrates **5a-c** and (b) achiral substrate **5c** with catalysts **1-4**. [a]50 mM phosphate buffer, pH 7.50; [b]100 mM phosphate buffer, pD 8.00; [c]1:1 MeOD-d_4/100 mM phosphate buffer, pD 8.00; [d]1:1 MeOD-d_4/100 mM phosphate buffer, pD 5.00; [e]Product not observed by ^{1}H NMR spectroscopy or GC-MS. [f]A single trans product was exclusively formed; the relative stereochemistry at the 1-position (−Me/−*n*Pr) could not be unambiguously determined. Selectivity measurements have an estimated error of ≤ 3%.

these treatments, with a higher *trans* selectivity observed between Δ_4-**2** and (*R*)-**5a** (*trans*/*cis*: 69/31, entry 3a) than with Δ_4-**2** and (*S*)-**5a** (*trans*/*cis*: 48/52, entry 2a). The averaged product *trans*/*cis* selectivity resulting from these treatments (58/42) is similar to that resulting from treatment of racemic **5a** with host (±)-**1** (65/35, entry 1a). In order to achieve similar levels of conversion under otherwise identical conditions, it was necessary for catalyst loadings of Δ_4-**2** to vary by a factor of two between treatments of (*R*)-**5a** and (*S*)-**5a**, an observation which suggests a moderate degree of recognition between Δ_4-**2** and enantiomers of **5a**. Likewise,

trans/*cis* ratios were within error between treatments of (±)-**1** or Δ_4-**2** with **5c**, although a difference in selectivity between (±)-**3** and Λ_4-**4** (entries 4a and 5a) with substrate (±)-**5a** was observed for reasons that are unclear. Nonetheless, in the majority of trials completed, varying the host chelator did not affect product selectivities by more than a small margin.

Next, product distributions from naphthalene-based catalysts were compared to those resulting from treatment with larger pyrene analogues (±)-**3** and **4**. In contrast to the selectivity observed from catalysis by Δ_4-**2**, treatment of **5c** with pyrene-based Λ_4-**4** resulted in the rapid formation of *trans* product with high selectivity (*trans*/*cis*: 98/2: entry 4b), demonstrating that increasing host cavity size through the use of a larger spacer can enhance stereoselectivity for *trans* products. In contrast, the high *trans* selectivities in entries 8a and 9a reflect the stereochemical preference of substrate **5b** due to a substantial 1,3-diaxial repulsion. When corrected for catalyst concentration, cyclization of **5c** by Λ_4-**4** proceeds more efficiently than that of Δ_4-**2** based on pseudo-first-order fits to the levels of conversion presented in Scheme 1 ($k_{rel} \approx 5$; $\Delta\Delta G^{\ddagger} = 1$ kcal·mol^{-1}). This preference for *trans* products was also observed between treatment of (±)-**5a** with naphthalene host (±)-**1** and pyrene analogues (±)-**3** and Λ_4-**4** (entries 1a, 4a and 5a). From these results, it is clear that exchanging a naphthalene for a pyrene spacer can affect a change in product diastereoselectivity that is consistent among different substrates (**5a,c**), as well as different hosts ((±)-**3,** Λ_4-**4**).

Collectively these observations suggest that the nature of chelator (CAM or TAM) used has little effect on the diastereoselectivity of this reaction. An exception to this trend results when the enantiopure hosts Δ_4-**2** or Δ_4-**4** interact in a diastereomeric fashion with substrate enantiomers (*i.e*. (*S*)- and (*R)*-**5a**). In contrast, the choice of spacer has a clear effect on product distributions, as is apparent from product selectivities resulting from treatment of **5a-c** with hosts (±)-**1** and **2** compared to (±)-**3** and **4**. Generally, it was observed that *trans* selectivity increases with cavity size, which may also accompany an improvement in catalytic efficiency. Consistent with these observations, gas-phase DFT calculations suggest that the barrier for the cyclization of **5a** is slightly lower for the transition state leading to the major *trans* product compared to that leading to the corresponding *cis* product.[40] Based on these results, it is likely that the constrictive cavities of (±)-**1** and **2** may destabilize the transition state leading to *trans* products, an effect that also results in higher selectivity for *cis* products relative to analogous reactions in larger hosts (±)-**3** and **4**.

Effect of host and guest size on enantioselective catalysis. The relationship between guest volume and catalyst enantioselectivity was investigated in the kinetic resolution of chiral starting material. In a catalytic kinetic resolution, the relative reaction rates of substrate enantiomers can be expressed as a selectivity factor (*s*; *eq*. 1),[44] which is determined by $\Delta\Delta G^{\ddagger}$ between diastereomeric transition states. It was hypothesized that if the size of substrates was increased, an increase in *s* may be observed due to increased steric interactions between encapsulated substrate and the aromatic walls of Λ_4-**2**, which are presumably the surfaces that induce enantioselectivity in these reactions.[31,38]

$$s = \frac{k_{fast}}{k_{slow}} = e^{\frac{\Delta\Delta G\ddagger}{RT}} \qquad (1)$$

Toward this end, selectivity factors were measured for chiral starting materials **5a** and **5b** (1:1 MeOD-d_4/100 mM phosphate buffer cosolvent, pD 5.00, 25 ^{0}C). While Λ_4-**2** exhibited low chiral discrimination for **5a** (s = 1.8; $\Delta\Delta G^{\ddagger}$ = 0.35 kcal·mol^{-1}), selectivity increased for larger substrate **5b** (s = 4.45; $\Delta\Delta G^{\ddagger}$ = 0.88 kcal·mol^{-1}). Following this observation, product ee's resulting from the cyclization of **5c** with hosts Δ_4-**2** and Λ_4-**4** were compared. In the latter case, an analogous trend was observed; product enantioselectivity was greater when a smaller cavity was used (entry 2b, 61% ee; $\Delta\Delta G^{\ddagger}$ = 1.14 kcal·mol^{-1}; Scheme 1)[31] relative to a larger one (entry 4b, −33% ee; $\Delta\Delta G^{\ddagger}$ = 0.56 kcal·mol^{-1}; Scheme 1). In further support of this notion, a smaller degree of recognition (indicated by small differences in product selectivity and conversion) was observed between enantiomers of **5a** and host Δ_4-**4** (entries 6a and 7a) compared to analogous trials with smaller host Δ_4-**2** (entries 2a and 3a). While these observations are consistent with the notion that the magnitude of host-mediated enantioinduction increases with guest size (or decreases with host cavity size), it should be noted an analogous trend was not observed between two previously reported achiral Prins substrates.[31]

Mechanistic considerations. In order to determine the role of catalyst, substrate and bulk solution acidity on reaction rate, the order in (±)-**1**, **5c** and D^+ were determined using initial rate measurements (^{1}H NMR spectroscopy). Because this reaction proceeds initially by a reversible encapsulation pre-equilibrium, saturation of catalyst by substrate is possible in principle. In practice, however, saturation by **5c** was not observed due to the low affinity of this substrate for (±)-**1** or **2** and the limited solubility of substrate in MeOD-d_4/phosphate buffer cosolvent. Consequently, the rate of reaction was measured to be first-order in (±)-**1** as well as substrate **5c**. In contrast, a 0.4(1)-order dependence was measured between k_{obs} and D^+ over the pD range 6.9-8.0. Taken together, these experiments demonstrate that the (±)-**1**-catalyzed cyclization of **5c** obeys the empirical rate law: rate = k_{obs}[substrate][host][D^+]$^{0.4(1)}$, which at constant pD reduces to rate = k_{obs}[substrate][host]. These measurements and subsequent observations described below are consistent with the mechanisms proposed in Scheme 2.

Investigation of the catalytic steps

Aldehyde-hydrate (K_{hyd}) and encapsulation (K_1) pre-equilibria. Under aqueous conditions, aldehyde-containing substrates underwent reversible hydration, a process which was observed by ^{1}H NMR spectroscopy. Evidence for the assignment of the hydrate was obtained by varying the proportion of MeOD-d_4 to phosphate buffer cosolvent. While the hydrate C-*H* resonance was absent in pure MeOD-d_4, the ratio of hydrate to aldehyde integrals increased with increasing proportion of aqueous phosphate buffer. During these experiments, the sum of aldehyde to hydrate resonances remained constant and was equal to the sum of corresponding alkene C-*H* resonances. Extraction of this mixture into $CDCl_3$ and subsequent analysis by ^{1}H NMR spectroscopy resulted in the quantitative recovery of aldehyde, confirming that hydration is reversible. The magnitude of the aldehyde-hydrate ratio also varied considerably between substrates; the ratio of aldehyde to hydrate was lower for less hydrophobic substrates in aqueous solution.[45] Following these qualitative experiments, it was next investigated whether substrate-dependent K_{hyd} pre-equilibria could affect guest binding and catalysis.

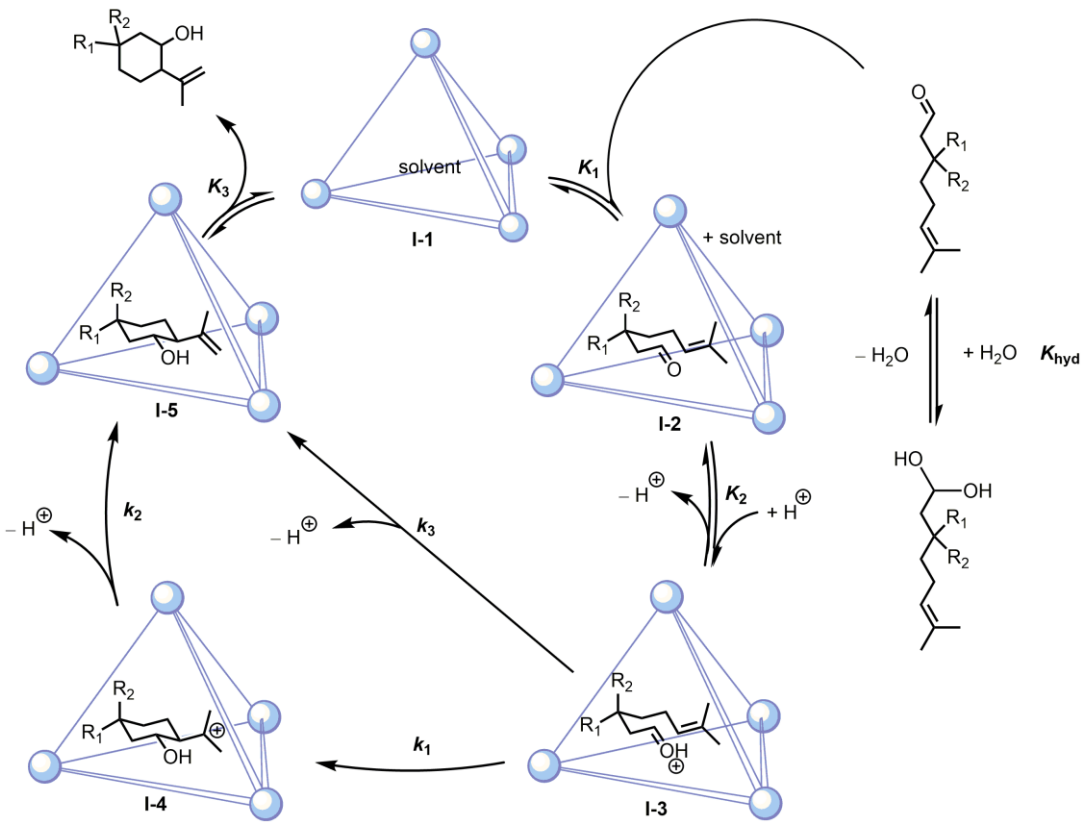

Scheme 2. Proposed mechanisms for host-catalyzed Prins cyclizations, where stepwise (k_1, k_2) or concerted (k_3) pathways are plausible.

To determine the influence of encapsulation on aldehyde-hydrate equilibria, homogenous solutions of (±)-**5a** and **5c** were treated with host (±)-**1**. ^{1}H NMR analysis revealed significant broadening of aldehyde C-*H* resonances, indicating guest exchange.[33,46,47] In contrast, hydrate resonances underwent no such broadening, indicating a negligible degree of encapsulation between hydrates of **(±)-5a**, **5c** and (±)-**1**. This result is attributable to the higher solvation of hydrate compared to aldehyde in the aqueous cosolvent employed. Increasing the ratio of (±)-**1** to **5c** resulted in an increase in the integrals of the encapsulated aldehyde resonances, accompanied by a decrease in the integral of the corresponding unencapsulated aldehyde resonance and R(OH)$_2$C-*H* hydrate resonance. These results confirm that encapsulation perturbs the aldehyde-hydrate equilibrium by selective encapsulation of aldehyde over hydrate.

It was hypothesized that the encapsulation of substrate aldehyde is driven by the hydrophobic effect, a process that has been shown to be controlled entropically by the release of encapsulated solvent.[48,49] In order to examine this effect, the influence of organic cosolvent on catalysis was investigated. Previously, the use of organic cosolvents had been observed to inhibit the (±)-**1**-catalyzed hydrolysis of orthoformates, an effect which results from the lower affinity of host and guest in nonaqueous solvents due to attenuation of the hydrophobic effect.[46,50,51] In contrast to purely aqueous conditions where the appearance of broad upfield resonances confirms a comparably high degree of guest association, guest binding is attenuated in a 1:1 (*v*/*v*) aqueous phosphate buffer/MeOD-d_4 cosolvent. Under homogenous conditions, encapsulated aldehyde, unencapsulated aldehyde and total host concentrations were measured

against an internal standard, from which dissociation constants were calculated (see K_M values, Table 1.).

In spite of the low magnitudes of association between host and substrate while using this cosolvent, catalysis in a 1:1 MeOD-d_4/phosphate buffer proceeded with an efficiency similar to that observed under pure aqueous buffer conditions. Catalysis did not proceed in pure methanol under otherwise identical conditions. The maintenance of catalytic efficiency in this cosolvent can be attributed in part to the higher concentrations of soluble guest in homogenous solutions, which, to some extent, offsets the lower degree of association observed. These experiments collectively suggest that host-catalyzed Prins cyclizations proceed initially through the displacement of solvent from the host cavity by substrate, an event that is driven by the hydrophobic effect.

Protonation of aldehyde oxygen (K_2), nucleophilic capture by alkene (k_1) and proton elimination (k_2); concerted pathway (k_3). After encapsulation, we propose that the host activates the substrate by stabilization of its conjugate acid, driving protonation of the carbonyl oxygen, followed by intramolecular nucleophilic attack by the pendant alkene. In principle, protonation of the carbonyl could occur prior to encapsulation. However, the latter scenario seems unlikely based on prior studies where the catalytic resting states for (±)-**1**-mediated orthoformate hydrolysis and Nazarov cyclizations were identified as the neutral guest species, whose ether- and alcohol-based oxygen atoms have a basicity similar to those of carbonyl oxygen functionalities.[33,52] To examine equilibrium K_2, the rate of cyclization of **5c** by (±)-**1** was measured to be slightly nonlinear between pD 6.9 and 8.0. Over this range, the dependence of k_{obs} on bulk solution was approximately 0.4(1)-order. This result bears analogy to the 0.5(1)-order relationship between k_{obs} and pD previously measured in the **1**-catalyzed Nazarov cyclization.[52] Because the aldehyde-hydrate equilibrium was perturbed slightly toward aldehyde at lower pD in the Prins reactions, the less than first-order dependence could not be due to a bulk solution effect on this pre-equilibrium.[53–55] These observations suggest that host-catalyzed Prins reactions are only indirectly promoted by increasing acidity of the bulk solution, a result that is inconsistent with a mechanism that proceeds exclusively through specific acid catalysis by D_3O^+. General acid catalysis could be operative, wherein the changes in k_{obs} with D^+ may correlate with the pK_a of a general acid involved in catalysis. In principle, a gallium-bound catecholamide functionality could act as a general acid catalyst in this regard.[56,57] These measurements suggest that host-catalyzed Prins reactions are promoted by bulk solution acidity, albeit in a complex manner.

Previous investigations have demonstrated that (±)-**1** can enforce a chair conformation of acyclic guests.[51,58,59] Based on this precedent, it is likely that cyclization is accelerated by steric constraints afforded through encapsulation. Following protonation of the encapsulated substrate, cyclization could conceivably proceed through either a step-wise (k_1, k_2) or concerted (k_3; Scheme 2) pathway. These mechanisms could, in principle, be distinguished by the direct observation of carbocation **I-4** (Scheme 2). However, under the catalytic conditions employed, guest binding is too weak to permit the definitive characterization of this possible species. To address whether a stepwise or concerted pathway was likely operative in host-catalyzed cyclizations, prior mechanistic investigations of **5a** cyclizations were consulted. Under anhydrous Lewis acidic conditions, the cyclization of **5a** is thought to proceed through a concerted mechanism and results in *trans* or *cis* products, depending on the nature of the catalyst.[59–61] In contrast, Brønsted acid-catalyzed cyclizations proceeding under either aqueous or anhydrous conditions have been shown to afford predominantly *cis* products resulting from

nucleophilic capture of carbocation **I-4**.[40,62–65] It has been suggested that the *cis* selectivity in the latter cases results from ion pairing with carbocation **I-4**, which would stabilize this intermediate, leading to products of nucleophilic capture by water or anion.[64] In support of this notion, a Lewis acid catalyst reported by Kočovský *et al*. afforded ene products under anhydrous conditions, but diols were observed when trace amounts of water were present in the reaction mixture.[66] DFT calculations have also suggested that the preference for *trans* over *cis* ene products for **5a** cyclization decreases when moving from concerted to stepwise mechanisms.[40] These studies suggested to us that the presence of water or an appropriate anion could, by stabilizing a carbocation intermediate, influence not only product chemoselectivity, but diastereoselectivity as well.

Based on these reports, it was unclear whether the exclusion of water during host-catalyzed Prins cyclizations of **5a** could explain the observed *trans* product diastereoselectivity. This stereoselectivity is unlikely to have resulted from constrained steric interactions, as increased steric confinement has been shown to accompany increased *cis* product selectivity (see Scheme 1). To probe whether a low concentration of water in the host cavity could account for the observed *trans* diastereoselectivity, **5a** was treated with various MeOH/100 mM aqueous phosphate buffer (pH 3.20) cosolvents in the absence of host, where the volumetric ratio of MeOH to buffer varied between 0 and 1.5. After heating, products were extracted and analyzed by ^{1}H NMR spectroscopy. While the proportions of alkene products formed from these treatments were minor (10-20% product selectivity), the *trans* selectivity of these products increased monotonically with an increasing proportion of MeOH (at 0% MeOH, *trans*/*cis* = 0.84; at 60% MeOH, *trans*/*cis* = 1.56). We speculate that this correlation between an increasing ratio of MeOH and *trans* product selectivity results from the destabilization of a stepwise cyclization mechanism in the presence of a lower dielectric bulk cosolvent. In principle, this change in mechanism could be accomplished through lowering the effective concentration of water in bulk solution, the absence of which would conceivably destabilize the stepwise transition state leading to *cis* products. Based on these experiments, it is possible that host-catalyzed cyclizations may be more concerted in character than stepwise processes occurring under conventional Brønsted acid catalysis. Furthermore, simply the exclusion of water from the host cavity during catalysis could account for the observed *trans* product selectivity.

Product displacement and turnover (K_3). In order to test whether cyclization was reversible under the reaction conditions employed, a mixture of alkene products (±)-**6-9a** was treated with an aqueous solution of (±)-**1** (7 mM, 8 mol %) and subjected to heating. After extraction, no starting material (±)-**5a** or changes in product distribution were observed, suggesting that catalysis is irreversible under catalytically relevant conditions.

Although product inhibition is a common challenge in cavity-mediated catalysis,[67–73] no deviation from first-order kinetics was seen through 90% conversion of **5c** with 4 mol % Λ_4-**2**, an observation which demonstrates that inhibition is largely negligible and implies that $K_1 > K_{-3}$. It was hypothesized that the absence of product inhibition results from the high solvation of product alcohol by the bulk solution. In this instance, the higher degree of product solvation compared to that of the starting material could provide a driving force for turnover. Consistent with this notion, the water solubility of **5a** (0.9 mM) is lower than that of (−)-menthol (4.0 mM) by a factor of 4.4.[74] In order to test the effect of the alcohol functionality on encapsulation and catalysis, a stock solution of (±)-**1** was partitioned to two identical reaction flasks which were treated with an equimolar stock solution of either (−)-menthol or (−)-menthyl chloride in an aqueous methanolic cosolvent. ^{1}H NMR analysis revealed that, although

encapsulation was evident for (−)-menthyl chloride, no encapsulation was observed for (−)-menthol. This observation attests to the importance of alcohol hydrogen bonding in guest solvation and consequently, host-substrate affinity. These mixtures were treated with equal concentrations of (±)-**5a** and heated, after which the organic portions were extracted and first-order rate constants determined based on the level of conversion the starting material had undergone. From these measurements, a small but measurable degree of catalytic inhibition was observed for the (−)-menthyl chloride case relative to the condition with (−)-menthol (k_{rel} = 0.7(1)). Consequently, it is conceivable that the formation of alcohol-containing products from aldehyde-containing starting materials drives turnover through a preferential hydrogen bonding interaction between product and aqueous solvent, a trait that correlates with the greater solubility of alcohol-containing products compared to aldehyde-containing starting materials. Combined with the high thermal persistence of **2**, this catalytic property allows for high turnover numbers to be achieved. Under dilute conditions (0.049 mM, 0.045 mol % Λ_4-**2**), catalysis proceeded with up to 840 turnovers over two weeks, which is among the highest reported for intramolecular Prins or carbonyl-ene cyclizations.[60,75–79]

$$S + H \underset{k_{-1}}{\overset{k_1}{\rightleftharpoons}} S{\subset}H \xrightarrow{k_{cat}} P + H \qquad (2)$$

$$\frac{d[P]}{dt} = \frac{k_{cat}[H][S]}{[S] + K_M} \qquad (3)$$

$$K_M = \frac{k_{cat} + k_{-1}}{k_1} \qquad (4)$$

Table 1. Kinetic Parameters for Host-catalyzed Prins Reactions

entry	substrate	catalyst	K_M (mM)	k_{cat} (s^{-1})	k_{cat}/K_M ($M^{-1}\cdot s^{-1}$)	$(k_{cat}/K_M)/k_{uncat}$ (M^{-1})	k_{cat}/k_{uncat}
1	**5c**	(±)-**1**	5.4 x 10^2	8.9 x 10^{-4}	1.6 x 10^{-3}	2.9 x 10^4	1.6 x 10^4
2	**5c**	Λ_4-**2**	5.8 x 10^2	5.4 x 10^{-3}	9.3 x 10^{-3}	1.6 x 10^5	9.5 x 10^4
3	(±)-**5a**	(±)-**1**	2.0 x 10^2	5.5 x 10^{-4}	2.7 x 10^{-3}	2.5 x 10^5	5.0 x 10^4
4	(*S*)-**5a**	Δ_4-**2**	3.3 x 10^2	1.0 x 10^{-3}	3.0 x 10^{-3}	2.8 x 10^5	9.1 x 10^4
5	(*R*)-**5a**	Δ_4-**2**	1.8 x 10^2	2.1 x 10^{-3}	1.2 x 10^{-2}	1.1 x 10^6	1.9 x 10^5

k_{uncat} for **5c**: 5.7(6) x 10^{-8} s^{-1}; (*S*)-**5a**: 1.1(1) x 10^{-8} s^{-1}; K_M measurements have an estimated error of 10%; Conditions for all runs: 1:1 MeOD-d_4/100 mM phosphate buffer, pD 8.00; 25 °C.

Michaelis-Menten analysis, rate accelerations. The observation that host-substrate complexes undergo fast chemical exchange,[80] accompanied by a relatively slow rate of catalysis, implies a mechanism involving a fast pre-equilibrium including encapsulation followed by a rate-limiting process that was irreversible under the reaction conditions used (*eq*. 2). Based on these characteristics, guest-binding and subsequent catalytic steps were deconvoluted with Michaelis-Menten analysis. As mentioned previously, the cyclization of **5c** was measured to be first-order in substrate and (±)-**1**, both of which are consistent with the rate law given below (*eq*. 3).[81,82]

Because guest exchange is fast with respect to cyclization, experimentally determined $K_d = K_M$. Uncatalyzed cyclizations proceeded slowly; less than fifteen percent of starting materials (*S*)-**5a** and **5c** were observed to cyclize over the course of four weeks. Nonetheless, these low levels of conversion were sufficient to quantify the uncatalyzed rates of reaction in bulk solution. The experimental k_{uncat} for **5a** is roughly an order of magnitude faster than the calculated gas-phase value, a difference which can be accounted for by the stabilizing role of water on the calculated transition state.[83] Notably, the uncatalyzed cyclization of **5c** proceeds approximately five times faster than that of (*S*)-**5a**. The magnitude of this difference in rate is small compared to other examples of the *gem*-disubstituent effect.[84] In contrast, catalysis by **1**-**4** proceeds relatively quickly, with half-lives on the order of hours to a day, depending on the experimental conditions. Specificity factors (k_{cat}/K_M) were largest for (*R*)-**5a** and **5c** with host **2**. These properties are a reflection of (a) the generally higher rate of catalysis with **2** compared to (±)-**1**, (b) the slightly more hydrophobic nature of **5c** compared to **5a**, which favors encapsulation both through the hydrophobic effect and aldehyde-hydrate equilibria, and (c) the complementarity of the (*R*)-**5a**/Δ_4-**2** diastereomeric pairing in catalysis. Catalytic proficiencies ((k_{cat}/K_M)/k_{uncat}), as measures of transition state stabilization afforded through encapsulation relative to the uncatalyzed reactions, were consistently higher for less hydrophobic substrates (*R*)-, (*S*)- and (±)-**5a**. This trend is a reflection of the tendency for host to drive substrate cyclization through the selective encapsulation of aldehyde over hydrate. In the case of (*S*)-**5a**, k_{uncat} is low in part due to the relatively hydrate-favored aldehyde-hydrate equilibrium. The tendency for hosts to compensate for the *gem*-disubstituent effect also likely contributes to this trend.[24] Catalytic rates (k_{cat}) for all substrates were consistently higher in **2** than (±)-**1** by less than an order of magnitude. On the whole, rate accelerations ranged between 10^4 and 10^5 (5.7-7.2 kcal·mol^{-1}), the latter of which are among the largest observed with a synthetic supramolecular cavity.[69,85-90]

Conclusion

While variation in the host chelator was generally observed to produce no significant changes in product selectivity, catalysis in TAM-based **2** proceeded with consistently higher efficiency than CAM-based (±)-**1**. In contrast, variation in host spacer (Nap or Pyr) resulted in changes in efficiency and product selectivity. Up to 840 turnovers were observed, which numbers among the highest known for intramolecular Prins cyclizations. Rate accelerations for the catalyzed reactions are on the order of 10^4-10^5 relative to uncatalyzed treatments, which are likewise among the highest reported in the field of host-guest catalysis. The trends reported herein enable a better understanding of enzyme-mimic microenvironment in the context of chemo-, diastereo- or enantioselective catalysis. In a broader sense, this work aims to build a fundamental understanding of biological catalysts using simple synthetic models.

Experimental Procedures. Unless otherwise noted, reactions and manipulations were performed using standard Schlenk techniques or in an oxygen-free wet box under nitrogen atmosphere. All solvents were degassed under nitrogen for 20 min before use. Glassware was dried in an oven at 150 °C overnight or by flame before use. Column chromatography was carried out

on a Biotage SP1 MPLC instrument with prepacked silica gel columns. NMR spectra were obtained on a Bruker AV 400 (400 MHz), AV 500 (500 MHz) or AV 600 (600 MHz) spectrometer. Chemical shifts are reported as δ in parts per million (ppm) relative to residual protiated solvent resonances. NMR data are reported according to the format s = singlet, d = doublet, t = triplet, m = multiplet, b = broad; integration; coupling constant. Mass spectral data were obtained at the QB3 Mass Spectrometry Facility operated by the College of Chemistry, University of California, Berkeley. Electrospray ionization (ESI) mass spectra were recorded on a Finnigan LTQ FT mass spectrometer. Chiral GC analyses were conducted using a HP 6850 series GC system fitted with a chiral column, BetaDex 120 Fused Silica Capillary Column (30 m x 0.25 mm x 0.25 um film thickness). Unless otherwise noted, chemicals were obtained from commercial suppliers and used without further purification. Preparations of **1**, **2** and **5c** have been described.[24,31] Compound **3** was prepared by the route previously reported[36] and precipitated with acetone. Unless otherwise noted, reported pD values are uncorrected for the glassy electrode artifact (*i.e.* $pD_{corr} = pD_{read} + 0.40$).[91]

General preparation of (6-11) used for selectivity determination and ee determination of starting material and product. This procedure is adapted from earlier reports.[24,31] Aldehyde starting material (45 μmol), **1**, **2, 3** or **4** (4.2 μmol), 250 μL MeOD-d_4 and 250 μL phosphate buffer (for example, 100 mM K_2DPO_4, pD 8.00) were added to a standard NMR tube. This slightly heterogeneous mixture was heated in an oil bath for a period of time as indicated, after which the organic components were extracted (3 x 300 μL $CDCl_3$) and passed through a pipet containing a thin filter of glass fiber. Selectivity and conversion were determined by ^{1}H NMR integration. *Cis* and *trans* product isomers were differentiated by characteristic alcohol C-*H* coupling[24] and accompanying alkene C-H resonances (*ca*. 4.9 ppm). GC-MS analysis of these samples confirmed the presence of only aldehyde starting material and alkene products. Products and starting material were isolated by silica gel chromatography (10% EtOAc in hexanes) prior to ee determination by chiral-GC and characterization. Selectivity factors were determined by direct rate measurement ((*R*)- and (*S*)-**5a**) or based on conversion and ee (**5b**), as described in reference 44. Turnover was assessed following treatment of Λ_4-**2** (7.0 mg, 0.0015 mmol) with **5c** (540 mg, 3.2 mmol) in 1:1 MeOH/100 mM phosphate buffer, pH 5.40 (30 mL, 13d 2h, 50 ^{0}C) and this heterogeneous mixture stirred vigorously, after which organic portions were extracted (3 x 30 mL DCM), dried over $MgSO_4$, solvent removed *in vacuo* and the combined yield of **10** and **11** assessed using an internal standard of mesitylene in $CDCl_3$ (38% yield, 1.2 mmol). Due to the elevated temperature and long reaction time employed, a modest amount of background reactivity was evident in the production of *p*-menthane-3,8-diols (~10% yield).[24] Treating a higher concentration of Λ_4-**2** (0.30 mM) with 530 equivalents of **5c** afforded 455 turnovers after 3 d and only trace (< 1% yield) *p*-menthane-3,8-diols. Characterization of *trans*-5-methyl-2-(prop-1-en-2-yl)-5-propylcyclohexan-1-ol (**8/9b**): ^{1}H NMR (600 MHz, $CDCl_3$): δ (ppm) 4.91 (s, 1H), 4.85 (s, 1H), 3.64 (dt, 1H), 1.90-1.76 (m, 2H), 1.75 (s, 3H), 1.35-1.45 (m, 2H), 1.23-1.35 (m, 6H), 1.09 (t, 2H), 0.90 (s, 3H), 0.85 (t, 3H); ^{13}C NMR (151 MHz, $CDCl_3$): δ (ppm) 146.96, 112.63, 67.76, 54.88, 48.93, 45.08, 36.92, 35.45, 25.58, 21.91, 19.07, 16.34, 14.49; HRMS (FTMS ESI) calculated for $[C_{13}H_{24}O]^+$: 196.1827; found:196.1824.

General procedure for rate measurements. In a typical experiment, a homogenous solution of aldehyde starting material (20 μmol), host **1** or **2** (2 μmol), 250 μL MeOD-d_4 and 250 μL 100 mM phosphate buffer (from K_3PO_4/HCl; pD 5.00 or 8.00) was prepared and added to a standard NMR tube. The tube was then inserted in a preheated NMR probe (25.0(1) ^{0}C) within three minutes of its preparation and the reaction followed with single scan ^{1}H experiments. In the case of more

slowly reacting substrate/host pairs, reactions were monitored every 1-2 h over the course of 8-10 h, from which initial rates (k_{obs}/mM·s^{-1}) were obtained. From these observed rates, k_{cat} values were calculated using initial substrate and host concentrations during catalysis and K_d, which was substituted for K_M in *eq. 2* in accordance with established procedure.[46,47] Due to the low affinity of host and guest, K_d values were obtained separately using higher concentrations of host (*ca.* 15 mM). Based on the observation that only aldehyde species (not hydrate) were encapsulated, the effective aldehyde concentration at the beginning of the run was treated as [*S*] in *eq. 3*. Quantitative mass balances of product and starting material were observed during kinetic trials. Background rates (k_{uncat}/s^{-1}) of cyclization were obtained by following an analogous procedure where solutions were monitored every 1-2 days over the course of a month. During initial trials it was observed that many internal standards had an inhibitory effect on catalysis, which presumably results from (a) internal or external association of the standard to the host and (b) the low affinity of the host for substrate in the cosolvent used. Consequently, rates of product formation were referenced against the residual MeOH solvent resonance, whose concentration was confirmed at the end of the kinetic run by the addition of an internal standard of 3-(trimethylsilyl)-1-propanesulfonic acid, sodium salt. Rates were reproducible within 10% among identically prepared solutions.

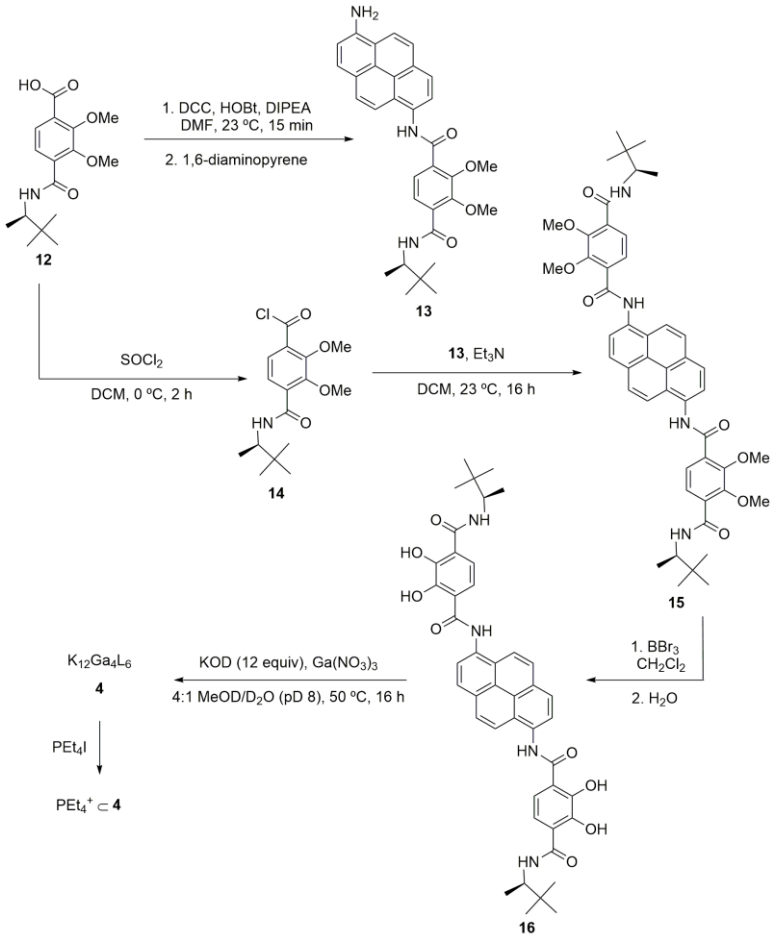

Scheme 3. Preparation of host **4**. For simplicity, only one ligand enantiomer is shown.

Preparation of 13: The previously-reported carboxylic acid **12**[31] (100 mg, 0.32 mmol) was dissolved in DMF (4 mL), and DCC (80 mg, 0.39 mmol) and HOBt (52 mg, 0.39 mmol) were added to the solution. The solution was stirred at ambient temperature for 30 minutes, and 1,6-diammoniumpyrene hydrogen sulfate (123 mg, 0.290 mmol) was added in one portion, followed by triethylamine (180 µL). The dark brown solution was stirred at ambient temperature for 16 h. A white solid was filtered off, and to the resulting solution was added H_2O (20 mL), forming a yellow precipitate. The suspension was filtered and washed with H_2O (3 x 2 mL). The precipitate was extracted with methylene chloride (25 mL) and the solvent evaporated to afford a yellow powder (**13**) that was used without further purification in the next step.

Preparation of 15: To a solution of carboxylic acid **12** (148 mg, 0.48 mmol) in methylene chloride (7 mL) at 0 ºC was added thionyl chloride (0.4 mL). The reaction mixture was stirred at 0 ºC for 2 h. After that time, volatile materials were removed *in vacuo* to afford a tan oil. Methylene chloride (2 x 2 mL) was added and evaporated to afford the acid chloride **14** as a colorless powder, which was used without further purification. **14** was added to a solution of **13** and triethylamine (0.180 mL, 1.28 mmol) in DCM (7 mL) at ambient temperature, and the resulting yellow solution was stirred for 40 h at ambient temperature. This yellow solution was diluted with DCM (50 mL) and washed with aqueous HCl (1N, 2 x 20 mL), aqueous NaOH (1N, 2x 20 mL), and brine (1 x 20 mL), and dried over Na_2SO_4. Solvent was removed and the resulting yellow powder reprecipitated from DCM/hexanes to afford **15** (130 mg, 51%) as a yellow powder. ^{1}H NMR (600 MHz, $CDCl_3$) ∂ (ppm) 10.71 (s, 2H), 8.91 (d, *J* = 8.4 Hz, 2H), 8.19 (d, *J* = 8.3 Hz, 2H), 8.15 (d, *J* = 8.3 Hz, 2H), 8.09 (q, *J* = 9.2 Hz, 4H), 8.02 (d, *J* = 8.4 Hz, 2H), 7.86 (d, *J* = 9.4 Hz, 2H), 4.25 (s, 6H), 4.17 (dq, *J* = 9.5, 6.8 Hz, 2H), 4.12 (s, 3H), 1.23 (d, *J* = 6.7 Hz, 6H), 1.04 (s, 18H). ^{13}C NMR (151 MHz, $CDCl_3$) ∂ (ppm) 163.44, 162.66, 151.65, 151.48, 131.69, 131.42, 129.73, 128.39, 128.28, 127.12, 127.09, 125.58, 125.54, 122.61, 121.35, 118.79, 62.52, 62.12, 53.55, 34.45, 26.53, 16.28. HRMS (FTMS ESI) calculated for $[C_{48}H_{54}N_4O_8]^+$: 815.3942, found 815.4017.

Preparation of 16: To a suspension of **15** (82 mg, 0.10 mmol) in methylene chloride (4 mL) was added BBr_3 (0.076 mL, 0.80 mmol). The yellow suspension instantly turned orange and was stirred at ambient temperature for 16 h. The suspension was then poured over ice and warmed to ambient temperature. The suspension was filtered to give a yellow solid that was suspended in water (10 mL). The yellow suspension was heated at reflux for 16 h and then cooled to ambient temperature. The mixture was filtered to afford **16** (55 mg, 72%) as a fine yellow powder. ^{1}H NMR (500 MHz, DMSO-d_6) ∂ (ppm) 12.87 (s, 2H), 12.15 (s, 2H), 11.30 (s, 2H), 8.51 (d, *J* = 9.0 Hz, 2H), 8.46 (d, *J* = 8.4 Hz, 2H), 8.40 (d, *J* = 8.2 Hz, 2H), 8.28 (q, *J* = 9.3 Hz, 4H), 7.72 (d, *J* = 8.6 Hz, 2H), 7.65 (d, *J* = 9.4 Hz, 2H), 4.11 – 4.03 (m, 2H), 1.16 (d, *J* = 6.9 Hz, 6H), 0.95 (s, 18H). ^{13}C NMR (126 MHz, DMSO-d_6, adduct with DCU) ∂ (ppm) 167.76, 167.03, 149.77, 148.63, 131.19, 128.71, 127.70, 125.29, 124.67, 124.44, 124.10, 121.42, 119.28, 118.19, 117.16, 52.52, 47.52, 34.67, 34.66, 33.34, 26.33, 26.29, 26.02, 25.32, 24.47, 15.34, 15.34. HRMS (FTMS ESI) calculated for $[C_{44}H_{46}N_4O_8 - H]^-$: 757.3243, found 757.3239.

Preparation of 4: In a glove box with a nitrogen atmosphere, KOD (3.52 mg, 0.064 mmol) was added to a suspension of **16** (24 mg, 0.032 mmol) in MeOD (0.64 mL), and the reaction mixture was stirred until the suspension became a homogeneous yellow solution. To this solution was added a 100 mM phosphate buffered solution of D_2O at pD = 8.0 (0.16 mL) and $Ga(NO_3)_3$ (5.44 mg, 0.021 mmol). The reaction mixture was heated at 55 ˚C for 14 h and subsequently cooled to ambient temperature and filtered. Solvent was removed to form a yellow solid, which was recrystallized from MeOH/Et_2O to afford **4** as a yellow solid (21 mg, 75%). ^{1}H NMR (500 MHz, MeOD) ∂ 14.00 (br, N*H*), 8.90 (br, 2H), 8.28 (br, 2H), 7.56 (br, 4H), 7.17 (br, 2H), 6.98 (br, 2H),

4.52 (br, 12H), 1.06 (d, J = 6.4 Hz, 36 H) 0.60 (s, 108 H). Upon addition of PEt_4I (5.5 mg, 0.02 mmol) to **4** in MeOD, encapsulation was observed within 15 minutes to afford $PEt_4^+ \subset$ **4** as one species. ^{1}H NMR (600 MHz, Methanol-d_4) ∂ (ppm) 14.30 (s, 7H), 11.59 (s, 12H), 9.09 (s, 12H), 8.49 (s, 12H), 7.80 (s, 12H), 7.65 (s, 12H), 7.26 – 7.20 (m, 12H), 7.09 (s, 12H), 4.60 (s, 12H), 1.14 (s, 81H), 0.68 (s, 115H), -3.10 – -3.25 (m, 20H). QTOF ES MS anion detection, m/z: 990.53 $[PEt_4^+ \subset H_6Ga_4L_6]^{5-}$.

Preparation of 5b. Propylmagnesium chloride (9.80 mL, 9.80 mmol, and 1.0 M solution in ether) was added drop wise to a solution of CuI (1876 mg, 9.80 mmol) in dry ether at -10˚C. The reaction mixture was cooled to −78˚C and (*E/Z*)-3,7-dimethyl-oct-2-enal (1500 mg, 9.80 mmol) was added drop-wise at this temperature. The resulting mixture was stirred for 1 h and slowly brought to room temperature. The mixture was washed with saturated NH_4Cl aqueous solution followed by brine solution and was extracted with ether. The combined organic layer was concentrated *in vacuo*. Flash chromatography on silica gel (10% ethyl acetate in hexanes eluant) afforded 130 mg (0.66 mmol, 7% yield) of the purified product 3-propyl-3,7-dimethyl-octanal **5b** as a yellow oil. ^{1}H NMR (600 MHz, $CDCl_3$): δ (ppm) 9.80 (t, 1H), 5.05 (t, 1H), 2.21 (d, 2H), 1.89 (q, 2H), 1.69 (s, 3H), 1.55 (s, 3H), 1.2-1.4 (m, 6H), 0.98 (s, 3H), 0.78 (t, 3H) ; ^{13}C NMR (151 MHz, $CDCl_3$): δ (ppm) 203.68, 131.45, 124.27, 52.79, 42.42, 40.02, 36.25, 25.62, 25.23, 22.24, 17.50, 16.75, 14.73; HRMS (FTMS ESI) calculated for $C_{13}H_{24}O$: 196.1827; found: 196.1830. Using two equivalents of propylmagnesium chloride in an analogous manner afforded a complex mixture instead of the desired 1,4-addition product.

References

(1) Reetz, M. T. *Proc. Natl. Acad. Sci. U. S. A.* **2004**, *101*, 5716–5722.
(2) Wombacher, R.; Keiper, S.; Suhm, S.; Serganov, A.; Patel, D. J.; Jäschke, A. *Angew. Chem. Int. Ed.* **2006**, *45*, 2469–2472.
(3) Klibanov, A. M. *Trends Biochem. Sci.* **1989**, *14*, 141–144.
(4) Margolin, A. L. *Enzyme Microb. Technol.* **1993**, *15*, 266–280.
(5) Reetz, M. T. *Angew. Chem. Int. Ed.* **2011**, *50*, 138–174.
(6) Croteau, R. *Chem Rev* **1987**, *87*, 929–954.
(7) Köksal, M.; Hu, H.; Coates, R. M.; Peters, R. J.; Christianson, D. W. *Nat. Chem. Biol.* **2011**, *7*, 431–433, and references therein (see The Dictionary of Natural Products, http://dnp.chemnetbase.com/; accessed Nov. 4, 2014).
(8) Cane, D. E. *Chem. Rev.* **1990**, *90*, 1089–1103.
(9) Blaszkiewicz, C.; Bricout, H.; Léonard, E.; Len, C.; Landy, D.; Cézard, C.; Djedaïni-Pilard, F.; Monflier, E.; Tilloy, S. *Chem. Commun.* **2013**, *49*, 6989–6991.
(10) Bassani, D. M.; Darcos, V.; Mahony, S.; Desvergne, J.-P. *J. Am. Chem. Soc.* **2000**, *122*, 8795–8796.
(11) Gianneschi, N. C.; Bertin, P. A.; Nguyen, S. T.; Mirkin, C. A.; Zakharov, L. N.; Rheingold, A. L. *J. Am. Chem. Soc.* **2003**, *125*, 10508–10509.
(12) Hooley, R. J.; Rebek Jr., J. *Chem. Biol.* **2009**, *16*, 255–264.
(13) Cacciapaglia, R.; Di Stefano, S.; Mandolini, L. *Acc. Chem. Res.* **2004**, *37*, 113–122.
(14) Pemberton, B. C.; Raghunathan, R.; Volla, S.; Sivaguru, J. *Chem. – Eur. J.* **2012**, *18*, 12178–12190.
(15) Pemberton, B. C.; Singh, R. K.; Johnson, A. C.; Jockusch, S.; Silva, J. P. D.; Ugrinov, A.; Turro, N. J.; Srivastava, D. K.; Sivaguru, J. *Chem. Commun.* **2011**, *47*, 6323–6325.
(16) Yoshizawa, M.; Klosterman, J. K.; Fujita, M. *Angew. Chem. Int. Ed.* **2009**, *48*, 3418–3438.

(17) Zhang, Q.; Tiefenbacher, K. *J. Am. Chem. Soc.* **2013**, *135*, 16213–16219.
(18) Hof, F.; Craig, S. L.; Nuckolls, C.; Rebek, Jr., J. *Angew. Chem. Int. Ed.* **2002**, *41*, 1488–1508.
(19) Breiner, B.; Clegg, J. K.; Nitschke, J. R. *Chem. Sci.* **2010**, *2*, 51–56.
(20) Kataev, E. A.; Müller, C. *Tetrahedron* **2014**, *70*, 137–167.
(21) Meeuwissen, J.; Reek, J. N. H. *Nat. Chem.* **2010**, *2*, 615–621.
(22) Sanders, J. K. M. *Chem. – Eur. J.* **1998**, *4*, 1378–1383.
(23) Raynal, M.; Ballester, P.; Vidal-Ferran, A.; van Leeuwen, P. W. N. M. *Chem. Soc. Rev.* **2014**, *43*, 1734-1787.
(24) Hart-Cooper, W. M.; Clary, K. N.; Toste, F. D.; Bergman, R. G.; Raymond, K. N. *J. Am. Chem. Soc.* **2012**, *134*, 17873–17876.
(25) Paschall, C. M.; Hasserodt, J.; Jones, T.; Lerner, R. A.; Janda, K. D.; Christianson, D. W. *Angew. Chem. Int. Ed.* **1999**, *38*, 1743–1747.
(26) Hasserodt, J.; Janda, K. D.; Lerner, R. A. *J. Am. Chem. Soc.* **1997**, *119*, 5993–5998.
(27) Hasserodt, J.; Janda, K. D.; Lerner, R. A. *J. Am. Chem. Soc.* **2000**, *122*, 40–45.
(28) Yoder, R. A.; Johnston, J. N. *Chem. Rev.* **2005**, *105*, 4730–4756.
(29) Siedenburg, G.; Jendrossek, D.; Breuer, M.; Juhl, B.; Pleiss, J.; Seitz, M.; Klebensberger, J.; Hauer, B. *Appl. Environ. Microbiol.* **2012**, *78*, 1055–1062.
(30) Hyatt, D. C.; Youn, B.; Zhao, Y.; Santhamma, B.; Coates, R. M.; Croteau, R. B.; Kang, C. *Proc. Natl. Acad. Sci.* **2007**, *104*, 5360–5365.
(31) Zhao, C.; Sun, Q.-F.; Hart-Cooper, W. M.; DiPasquale, A. G.; Toste, F. D.; Bergman, R. G.; Raymond, K. N. *J. Am. Chem. Soc.* **2013**, *135*, 18802–18805.
(32) Davis, A. V.; Fiedler, D.; Seeber, G.; Zahl, A.; van Eldik, R.; Raymond, K. N. *J. Am. Chem. Soc.* **2006**, *128*, 1324–1333.
(33) Pluth, M. D.; Bergman, R. G.; Raymond, K. N. *J. Am. Chem. Soc.* **2008**, *130*, 11423–11429.
(34) Merlau, M. L.; del Pilar Mejia, M.; Nguyen, S. T.; Hupp, J. T. *Angew. Chem.* **2001**, *113*, 4369–4372.
(35) Fiedler, D.; Leung, D. H.; Bergman, R. G.; Raymond, K. N. *Acc. Chem. Res.* **2005**, *38*, 349–358.
(36) Johnson, D. W.; Raymond, K. N. *Inorg. Chem.* **2001**, *40*, 5157–5161.
(37) Parac, T. N.; Caulder, D. L.; Raymond, K. N. *J. Am. Chem. Soc.* **1998**, *120*, 8003–8004.
(38) Brown, C. J.; Bergman, R. G.; Raymond, K. N. *J. Am. Chem. Soc.* **2009**, *131*, 17530–17531.
(39) Williams, J. T.; Bahia, P. S.; Snaith, J. S. *Org. Lett.* **2002**, *4*, 3727–3730.
(40) Williams, J. T.; Bahia, P. S.; Kariuki, B. M.; Spencer, N.; Philp, D.; Snaith, J. S. *J. Org. Chem.* **2006**, *71*, 2460–2471.
(41) Thomas, B. E.; Houk, K. N. *J. Am. Chem. Soc.* **1993**, *115*, 790–792.
(42) Terpin, A. J.; Ziegler, M.; Johnson, D. W.; Raymond, K. N. *Angew. Chem. Int. Ed.* **2001**, *40*, 157–160.
(43) Davis, A. V.; Fiedler, D.; Ziegler, M.; Terpin, A.; Raymond, K. N. *J. Am. Chem. Soc.* **2007**, *129*, 15354–15363.
(44) Keith, J. M.; Larrow, J. F.; Jacobsen, E. N. *Adv. Synth. Catal.* **2001**, *343*, 5–26.
(45) Gruen, L. C.; McTigue, P. T. *J. Chem. Soc. Resumed* **1963**, 5217–5223.
(46) Pluth, M. D.; Bergman, R. G.; Raymond, K. N. *J. Org. Chem.* **2009**, *74*, 58–63.
(47) Pluth, M. D.; Bergman, R. G.; Raymond, K. N. *Science* **2007**, *316*, 85–88.
(48) Breslow, R. *Acc. Chem. Res.* **1991**, *24*, 159–164.
(49) Leung, D. H.; Bergman, R. G.; Raymond, K. N. *J. Am. Chem. Soc.* **2008**, *130*, 2798–2805.
(50) Smithrud, D. B.; Diederich, F. *J. Am. Chem. Soc.* **1990**, *112*, 339–343.

(51) Biros, S. M.; Bergman, R. G.; Raymond, K. N. *J. Am. Chem. Soc.* **2007**, *129*, 12094–12095.
(52) Hastings, C. J.; Bergman, R. G.; Raymond, K. N. *Chem. – Eur. J.* **2014**, *20*, 3966-3973.
(53) Kurz, J. L.; Coburn, J. I. *J. Am. Chem. Soc.* **1967**, *89*, 3528–3537.
(54) Bell, R. P. In *Advances in Physical Organic Chemistry*; V. Gold, Ed.; Academic Press, 1966; Vol. Volume 4, pp. 1–29.
(55) Greenzaid, P. *J. Org. Chem.* **1973**, *38*, 3164–3167.
(56) Ji, C.; Peng, Y.; Huang, C.; Wang, N.; Luo, Z.; Jiang, Y. *J. Mol. Catal. Chem.* **2006**, *246*, 136–139.
(57) Yamada, Y. M. A.; Ikegami, S. *Tetrahedron Lett.* **2000**, *41*, 2165–2169.
(58) Dong, V. M.; Fiedler, D.; Carl, B.; Bergman, R. G.; Raymond, K. N. *J. Am. Chem. Soc.* **2006**, *128*, 14464–14465.
(59) Fiedler, D.; Bergman, R. G.; Raymond, K. N. *Angew. Chem.* **2004**, *116*, 6916–6919.
(60) Clarke, M. L.; France, M. B. *Tetrahedron* **2008**, *64*, 9003–9031.
(61) Nakatani, Y.; Kawashima, K. *Synthesis* **1978**, *1978*, 147–148.
(62) Cheng, H.; Meng, X.; Liu, R.; Hao, Y.; Yu, Y.; Cai, S.; Zhao, F. *Green Chem.* **2009**, *11*, 1227–1231.
(63) Yuasa, Y.; Tsuruta, H.; Yuasa, Y. *Org. Process Res. Dev.* **2000**, *4*, 159–161.
(64) Clark, B. C.; Chamblee, T. S.; Iacobucci, G. A. *J. Org. Chem.* **1984**, *49*, 4557–4559.
(65) Hayashi, E.; Hara, S.; Shirato, H.; Hatakeyama, T.; Fukuhara, T.; Yoneda, N. *Chem. Lett.* **1995**, *24*, 205–206.
(66) Kočovský, P.; Ahmed, G.; Šrogl, J.; Malkov, A. V.; Steele, J. *J. Org. Chem.* **1999**, *64*, 2765–2775.
(67) Jeong, K. S.; Go, Y. B.; Shin, S. M.; Lee, S. J.; Kim, J.; Yaghi, O. M.; Jeong, N. *Chem. Sci.* **2011**, *2*, 877.
(68) Reinhoudt, D. N.; Crego-Calama, M. *Science* **2002**, *295*, 2403–2407.
(69) Hastings, C. J.; Pluth, M. D.; Bergman, R. G.; Raymond, K. N. *J. Am. Chem. Soc.* **2010**, *132*, 6938–6940.
(70) Cacciapaglia, R.; Di Stefano, S.; Mandolini, L. *J. Am. Chem. Soc.* **2003**, *125*, 2224–2227.
(71) Koblenz, T. S.; Wassenaar, J.; Reek, J. N. H. *Chem. Soc. Rev.* **2008**, *37*, 247.
(72) Yoshizawa, M.; Tamura, M.; Fujita, M. *Science* **2006**, *312*, 251–254.
(73) Klöck, C.; Dsouza, R. N.; Nau, W. M. *Org. Lett.* **2009**, *11*, 2595–2598.
(74) Ajisaka, N.; Hara, K.; Mikuni, K.; Hara, K.; Hashimoto, H. *Biosci. Biotechnol. Biochem.* **2000**, *64*, 731–734.
(75) Yuan, Y.; Zhang, X.; Ding, K. *Angew. Chem. Int. Ed.* **2003**, *42*, 5478–5480.
(76) Evans, D. A.; Tregay, S. W.; Burgey, C. S.; Paras, N. A.; Vojkovsky, T. *J. Am. Chem. Soc.* **2000**, *122*, 7936–7943.
(77) Evans, D. A.; Burgey, C. S.; Paras, N. A.; Vojkovsky, T.; Tregay, S. W. *J. Am. Chem. Soc.* **1998**, *120*, 5824–5825.
(78) Grachan, M. L.; Tudge, M. T.; Jacobsen, E. N. *Angew. Chem.* **2008**, *120*, 1491–1494.
(79) Rueping, M.; Theissmann, T.; Kuenkel, A.; Koenigs, R. M. *Angew. Chem. Int. Ed.* **2008**, *47*, 6798–6801.
(80) Davis, A. V.; Raymond, K. N. *J. Am. Chem. Soc.* **2005**, *127*, 7912–7919.
(81) Michaelis, L.; Menten, M. *Biochem.* **1913**, 333–369.
(82) Michaelis, L.; Menten, M. L.; Johnson, K. A.; Goody, R. S. *Biochemistry (Mosc.)* **2011**, *50*, 8264–8269.

(83) Zardoost, M. R.; Gholami, M. R.; Irani, M.; Siadati, S. A. *Prog. React. Kinet. Mech.* **2012**, *37*, 173–182.
(84) Jung, M. E.; Piizzi, G. *Chem. Rev.* **2005**, *105*, 1735–1766.
(85) Molenveld, P.; Kapsabelis, S.; Engbersen, J. F. J.; Reinhoudt, D. N. *J. Am. Chem. Soc.* **1997**, *119*, 2948–2949.
(86) Saki, N.; Akkaya, E. U. *J. Mol. Catal. Chem.* **2004**, *219*, 227–232.
(87) Mock, W. L.; Irra, T. A.; Wepsiec, J. P.; Adhya, M. *J. Org. Chem.* **1989**, *54*, 5302–5308.
(88) Trainor, G. L.; Breslow, R. *J. Am. Chem. Soc.* **1981**, *103*, 154–158.
(89) Skouta, R.; Wei, S.; Breslow, R. *J. Am. Chem. Soc.* **2009**, *131*, 15604–15605.
(90) Marinescu, L. G.; Bols, M. *Angew. Chem. Int. Ed.* **2006**, *45*, 4590–4593.
(91) Glasoe, P. K.; Long, F. A. *J. Phys. Chem.* **1960**, *64*, 188–190.
(92) This chapter was adapted from Hart-Cooper, W. M.; Zhao, C.; Triano, R. M.; Yaghoubi, P.; Ozores, H. L.; Burford, K. N.; Toste, F. D.; Bergman, R. G.; Raymond, K. N. *Chem. Sci.* **2015**, *6* (2), 1383.

Chapter 4

Protein-like Proton Transfer in a Synthetic Active Site

Introduction

Water-mediated proton transfer in molecular cavities plays an essential role in the function of Nature's remarkable metabolic machinery.[1,2] Of the broad diversity of enzyme-catalyzed reactions, those involving hydrogen, proton or hydride (collectively, hydron) transfer are ubiquitous and of high fundamental importance.[3] For instance, ATP synthase employs an internal chain of water molecules to mediate proton transfer across an electrochemical gradient.[4,5] This process drives ATP synthesis, which allows organisms to broadly meet their basic energy needs. Recent studies of tunneling in enzymatic hydron transfer reactions have other far reaching and broad implications, namely the importance of the dynamic enzyme motions in driving catalysis.[6,7]

Of the methods used to study hydron transfer, kinetic studies of proton transfer through amide hydrogen deuterium exchange (HDX) have elucidated the dynamic interactions between water and protein surfaces that are central to the unique capabilities of enzymes.[8–13] Noncovalent interactions, such as electrostatic effects and hydrogen bonding, have also been shown to exert a significant influence on amide HDX rates. These properties are manifest in amide HDX rate constants that can vary by a factor of a billion for residues on the same protein.[8] How these variations arise, and how such a property could be harnessed to drive enzyme-like reactivity, remain challenging questions.

In a growing effort to emulate the efficacy of biological receptors and enzymes, studies of the preparative, guest-binding and catalytic properties of synthetic assemblies have been pursued.[14–21] While guest encapsulation has been reported in a variety of media, association processes of organic guests are generally more thermodynamically favorable in water.[22,23] Central to these studies is the notion that the displacement of a high-energy water cluster from a receptor drives guest association, and in some cases, subsequent catalysis. However, despite the abundance of structural data documenting diverse water clusters encapsulated in various host cavities, mechanistic descriptions of the dynamic processes between water and host are rare.[24–32]

As part of the broader field of synthetic hosts previously mentioned, our group has developed a class of biologically-inspired, anionic $K_{12}Ga_4L_6$ assemblies (e.g. **1**, Figure 1a).[33,34] Assembly **1** exhibits twelve intramolecular amide hydrogen bonds which, in analogy to structurally important peptide bonds found in polypeptides, preferentially stabilize the desired tetrahedral supramolecular structure over other conformers.[35] Compound **1** and related hosts have been shown to catalyze several important chemical reactions with sizable rate accelerations (up to 10^6) and unusual selectivity reminiscent of enzyme catalysis.[34,36–40] Unlike most enzymes, the reactions catalyzed by **1** are functionally and mechanistically very diverse. Despite these differences, those reactions proceeding with the largest rate enhancements in **1** all involve proton transfer steps. Spurred by this insight, we have investigated the fundamental mechanism of proton transfer in **1** through amide HDX kinetics. The purpose of these studies is twofold: first, to probe the fundamental mechanisms of acid, base and water-mediated proton transfer in a host that is known to promote enzyme-like rate accelerations in acid-mediated processes; second, to explore the effect of guest binding on proton exchange, which provides insight into the interplay of solvent and guest exchange for a synthetic active site. The results of these studies are broadly relevant to the ligand-receptor binding events involving biomacromolecules and the continued development of synthetic enzyme mimics that match or exceed the practical usefulness of their biological counterparts.

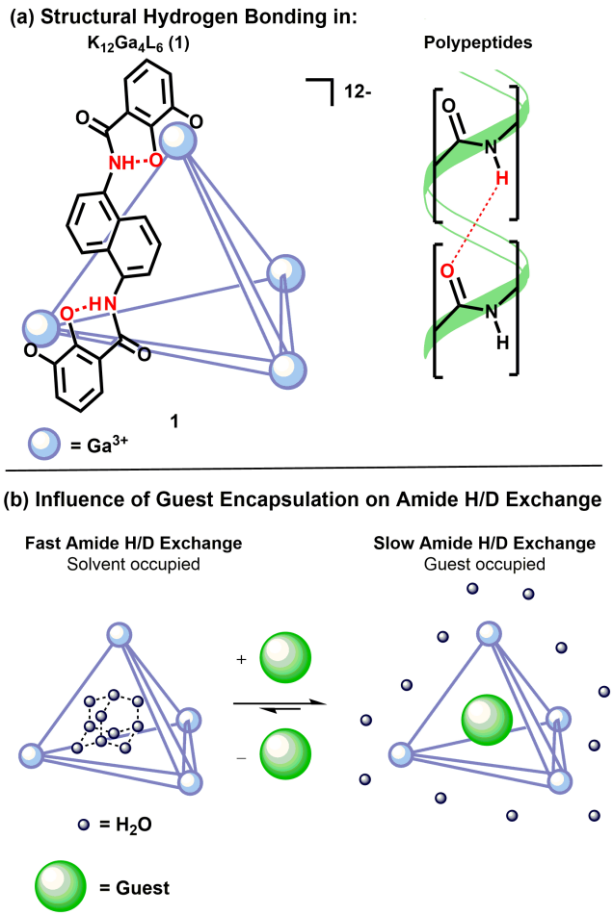

Figure 1. (a) Structurally important hydrogen bonding in a $K_{12}Ga_4L_6$ tetrahedron, **1** (lines represent ligands and spheres represent Ga^{3+} centers), and polypeptides. (b) General scheme of solvent displacement from **1** by a guest molecule.

Results and Discussion

Initial studies revealed a puzzling relationship between the observed rate of amide HDX and the identity of the encapsulated guest. In the absence of guest, ^{1}H NMR analysis revealed that **1** undergoes first-order amide H/D exchange relatively rapidly, as evidenced by the loss of a single protio amide resonance at 13.1 ppm (100 mM phosphate buffer, pD_{corr} 8.40, 25 ^{0}C; pD_{corr} reflects a pD value that is corrected for the glassy electrode artifact,[41] see experimental section). In the presence of a cationic guest, this rate decreased by a magnitude that is commensurate with the binding affinity of the host-guest pair. This relationship is represented in Figure 2, where at identical concentrations of host and excess guest, the log(k_{obs}) of amide HDX correlates linearly with log(K_a)[42] of the encapsulated guest. Thus, while it was clear that the presence of a strongly-

bound cationic guest inhibited host amide HDX, further investigations were necessary to explain this relationship.

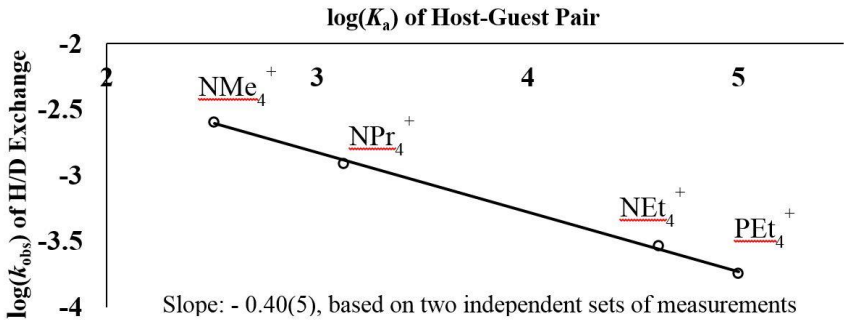

Figure 2. Linear free energy relationship between log(K_a) and log(k_{obs}) of amide HDX. All measurements were obtained using an excess (2 equiv.) of guest.

To probe the influence of guest encapsulation on the mechanism of amide HDX, **1** was treated with increasing concentrations of guest and H/D exchange rates were measured. In all cases, the rate of amide HDX decreased with increasing guest concentration until one equivalent of guest had been added (Figure 3). Increasing the concentration of added guest past one equivalent did not effect a decrease in k_{obs}, suggesting that a saturation limit in guest had been obtained and blocking the interior (but not exterior) of **1** strongly inhibits proton exchange. Eyring analysis revealed a large negative entropy of activation ($\Delta S^{\ddagger}$: -77(2) $J \cdot mol^{-1} \cdot K^{-1}$), which is similar to those of guest exchange.[43] Taken collectively, these data support an amide HDX mechanism proceeding by replacement of cationic guest by water, which is followed by proton exchange between encapsulated water and amide NH protons.

Based on these experiments, the guest-dependent amide HDX mechanism can be represented graphically in Figure 4 and described mathematically by *eq. 1*. In the absence of an inhibiting guest (**G** = NMe_4^+, NPr_4^+, NEt_4^+, PEt_4^+), the rate of HDX is k_2[**B**], where k_2 is directly measurable. However, when HDX is inhibited by the presence of an encapsulated guest (**G**), the rate of amide HDX competes with the process of guest exchange, the latter of which is correlated to the guest association constant (K_a; Figure 2).[43,44] Consequently, the rate of amide HDX decreases with increasing concentrations of guest until saturation is reached at a guest/host ratio of one, after which very little decrease in rate is observed and the rate approaches k_3[**A**]. As represented in Figure 4, the steps represented by k_2 and k_3 can be treated as irreversible, as reactions were measured in pure D_2O. In principle, association constants for **G** guests could conceivably differ between protio- and deutero-**1**. However, no deviations from first-order kinetics were observed in the conversion ranges measured, demonstrating that this effect is kinetically negligible in this context. This result is consistent with previous studies on the isotope effects of guest exchange and binding, where only small isotope effects were observed, even among considerably larger guests.[45,46] This description also provides a conceptual link between host-guest influenced HDX and the Linderstrøm-Lang model of structurally hindered proton exchange by proteins.[12,13] The

reduced flexibility of a host containing an alkylammoinium guest may also contribute to the observed inhibitory influence of guest concentration on HDX. Taken together, this model strongly supports the mechanisms described in Figure 4, where proton exchange proceeds quickly by the encapsulation of water, or slowly through direct exchange by the **G⊂1** complex with the surrounding aqueous medium.

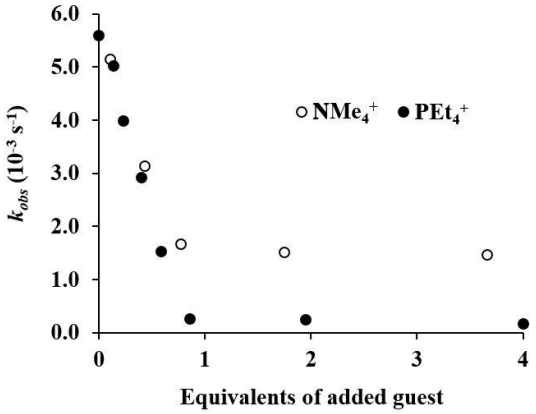

Figure 3. Effect of increasing guest equivalents on k_{obs} of amide HDX (pD_{corr} 8.40).

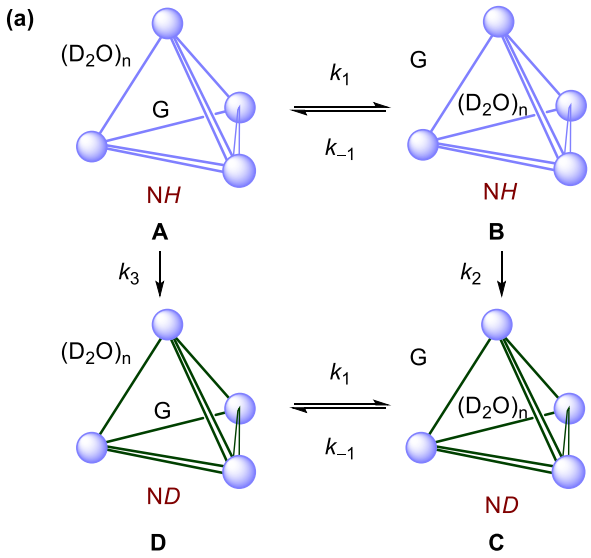

(b) $$k_{obs} = \left(\frac{k_1 k_2}{k_{-1}[G] + k_2} + k_3\right) f_A + k_2 f_B \quad (1)$$

Figure 4. (a) General guest-dependent mechanism for amide H/D exchange at constant pH and (b) rate law describing this process, where f_A and f_B are the fractions of host existing as A and B, respectively.

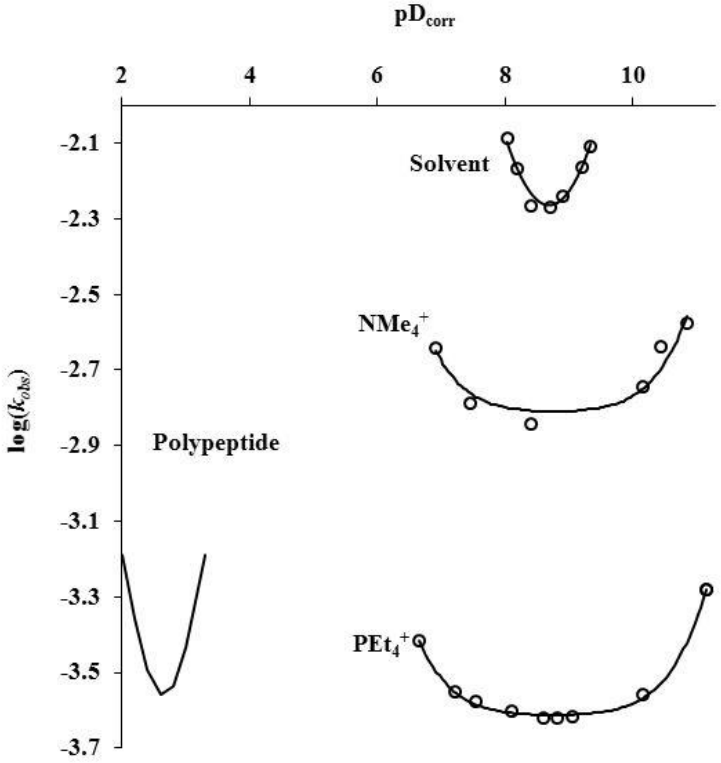

Figure 5. The influence of bulk solution pD_{corr} on k_{obs} of amide HDX. Varying the presence and type of guest affords order-of-magnitude changes in k_{obs}, whose minimum pD_{corr} values are shifted up to 6 pD units relative to model polypeptides reported in reference 8. Lines represent fits of experimental k_{obs} values to *eq. 2* (Figure 6d).

In order to assess the extent to which acid and base-mediated proton exchange processes are stabilized or destabilized in **1**, the effects of bulk solution pD_{corr} on HDX exchange rates were investigated. Mechanistic studies have revealed that amide HDX proceeds by acid, base, and to a lesser extent, neutral water-mediated mechanisms, of which the dominant mechanism is a consequence of bulk solution pH. This property is evident in the parabola-like relationship observed between log(k_{obs}) of amide HDX and bulk solution pD_{corr} (Figure 5). Control experiments demonstrated that proton exchange rates were insensitive to variation in KCl concentration and that guest exchange was invariant with changes in bulk solution pD_{corr}. Experimental rate constants obtained at variable pD_{corr} were fit to *eq. 2*, from which rate constants by acid (k_A), base (k_B) and water (k_W) were obtained. With simple polypeptides, the dominant mechanism of amide HDX switches over from acid- to base-catalysis between pH 2-4.[8] In **1**, however, this change in mechanism occurs around pH 9 indicating up to a million-fold shift in k_A and k_B relative to those of simple polypeptides. These dramatic differences demonstrate the high degree that pathway (a) is stabilized and pathway (b) is destabilized in **1** (Figures 5, 6; Table 1). We attribute this pH_{min} shift to local electrostatics resulting from the polyanionic nature of **1**, which is supported by studies of amide HDX in charged micelles.[4] In the presence of a guest (NMe_4^+ or PEt_4^+), the pD-dependent curves are flattened, implying that both acid and base-mediated exchange are preferentially

destabilized over the water-mediated pathways when the interior of **1** is blocked. Although the precise source of this effect cannot be known with certainty, we propose that encapsulated water stabilizes the charged intermediates of acid and base-mediated HDX (Figure 6a, b), which results in flattened curves when the host cavity is blocked. It is clear from these results that the local chemical environment of the exchanging amide hydrogen dramatically stabilizes an acid-mediated process over the corresponding base-catalyzed pathway. Furthermore, this environment can be perturbed by the presence of guest by orders of magnitude relative to solvent-filled **1**.

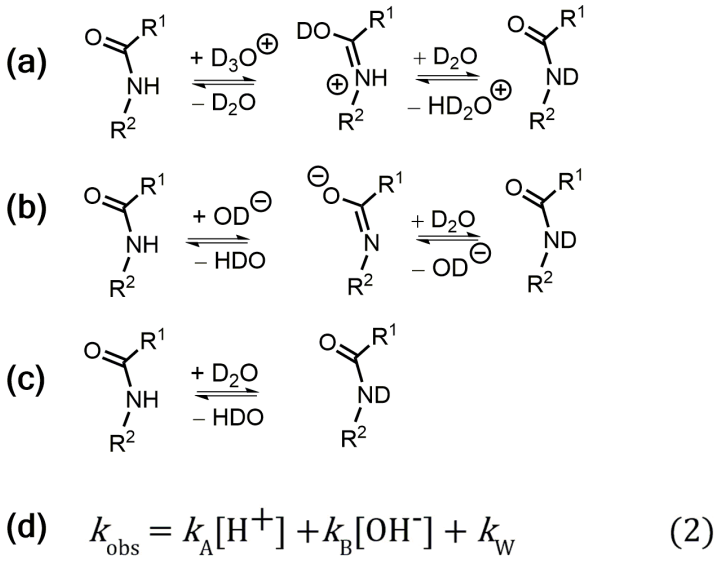

Figure 6. Acid (a), base (b) and water (c) mediated amide H/D exchange mechanisms, which, in the presence of a constant excess of guest **G** can be described by (d) *eq. 2*.

Table 1. Guest- and pD_{corr}-dependent kinetic parameters

	Guest		
	PEt_4^+	NMe_4^+	Solvent
$k_A/M^{-1}s^{-1}$	6.3 x 10^2	5.8 x 10^3	4.8 x 10^5
$k_B/ M^{-1}s^{-1}$	1.5	13	1.4 x 10^3
k_W/s^{-1}	2.4 x 10^{-4}	1.5 x 10^{-3}	3.4 x 10^{-3}

Conclusion

In summary, the observed rate of amide hydrogen-deuterium exchange (HDX) in a biologically inspired, anionic $K_{12}Ga_4L_6$ supramolecular assembly **1** was correlated to the affinity of alkylammonium and phosphonium cations for the host interior. Guest titration experiments confirmed that amide HDX proceeds through different mechanisms contingent on the presence or absence of a guest, justifying the above correlation and previous reports of cavity-mediated acid catalysis. The rates of HDX catalyzed by acid and base are shifted by a factor of a million relative

to those of polypeptides, an effect that we attribute to the polyanionic nature of **1**. Collectively, these experiments suggest that amide HDX occurs through encapsulation of water and the unique electrostatics of the host dramatically alters reactivity of this transient hydrate. These results improve our understanding of the role of water in host-guest association and describe an emergent mechanism of cavity-localized proton exchange. More broadly, these insights correlate processes of hydron transfer with enzyme-mimic activity, thereby providing a significant step toward the development of catalysts that may surpass the utility of biological enzymes.

Experimental

General procedures, instrumentation and materials. Unless otherwise noted, reactions and manipulations were performed using standard Schlenk techniques or in an oxygen-free wet box. NMR spectra were obtained on Bruker AV-500 or AV-600 spectrometers. Chemical shifts are reported as δ in parts per million (ppm) relative to residual protonated solvent resonances and an internal standard in all NMR experiments as indicated. Unless otherwise noted, chemicals were obtained from commercial suppliers and used without further purification. The synthesis of **1** and complexes with NMe_4^+, NPr_4^+, NEt_4^+ and PEt_4^+ have been described.[33,43] All solvents were degassed under N_2 for 20 min before use. Buffered solutions were made by titrating a K_3PO_4 solution with DCl until the desired pD was reached. Least squares fits were obtained using Origin (OriginLab, Northampton, MA). Reported pD_{corr} values are corrected for the glassy electrode artifact (*i.e.* $pD_{corr} = pH_{read} + 0.40$).[41] Association constants (K_a) for the encapsulation of NMe_4^+ ($\log(K_a/M^{-1}) = 2.51(1)$) and NPr_4^+ ($\log(K_a/M^{-1}) = 3.12(5)$) were measured by NMR, UV-vis and isothermal titration calorimetry.[42] The association constants for PEt_4^+ and NEt_4^+ have been previously reported.[42,43]

General procedure for amide HDX kinetic experiments. In a typical experiment, the CAM-nap host (5 mg, 1.4 μmol) was treated with a 0-5 equivalents of NMe_4Cl, NPr_4Br, NEt_4Cl or PEt_4I in H_2O. After 10 minutes, water was removed *in vacuo*, affording a yellow solid. This solid was then dissolved in 500 μL 100 mM deuterated phosphate buffer (from K_3PO_4/DCl; pD variable), after which the resulting solution was added to a standard NMR tube. The tube was then inserted in a preheated NMR probe (25.0(1) ^{0}C) and the reaction followed within three minutes of its preparation with single scan ^{1}H spectra acquired every 20-60 seconds. Decay of the amide N*H* resonance was assessed against the aromatic resonances of **1** and an internal standard of sodium 3-trimethylsilylpropanesulfonate, from which first-order fits were obtained. Reactions were followed for two to three half-lives and no deviations from first-order kinetics were observed. In the case of relatively fast conditions (e.g. HDX by solvent-filled host), rates were obtained from the last 20% conversion (see Figure 7). Large differences in KCl concentration, *i.e.* 20 and 570 mM, afforded no measurable change in HDX rate ($k_{rel} = 1.0(1)$), demonstrating that this salt does not influence the HDX mechanism. Guest exchange of PEt_4^+ for NEt_4^+ was likewise unaffected by moderate changes in bulk solution acidity (pD_{corr} 6.47 and 10.45; $k_{rel} = 1.1(1)$). Rates were reproducible within 5% among identically prepared solutions.

Representative time vs. concentration plot

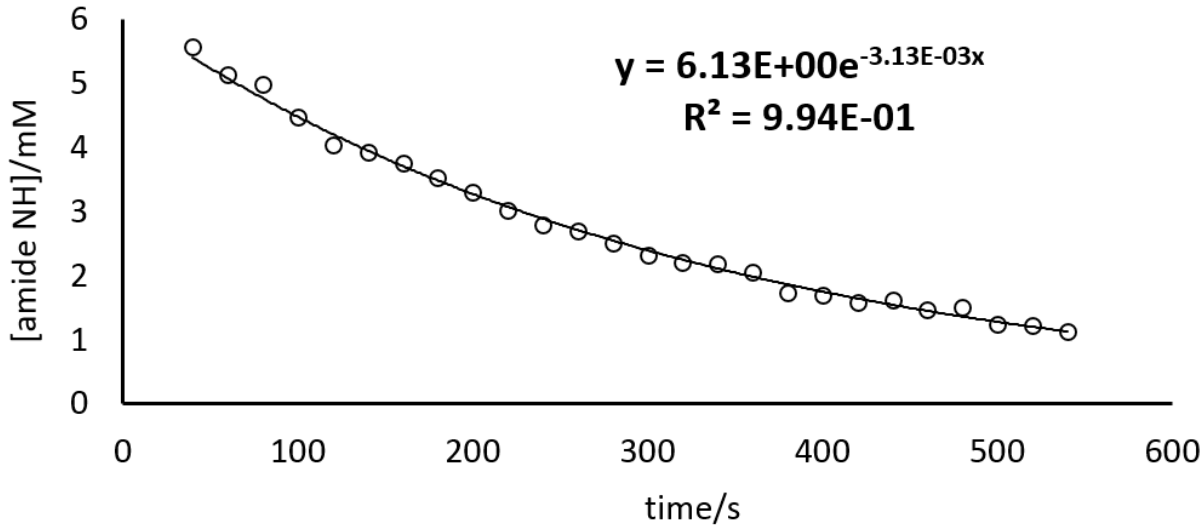

Figure 7. Typical concentration of amide N*H* versus time plot (guest = NMe_4^+).

Dependence of k_{obs} on temperature (Eyring plot)

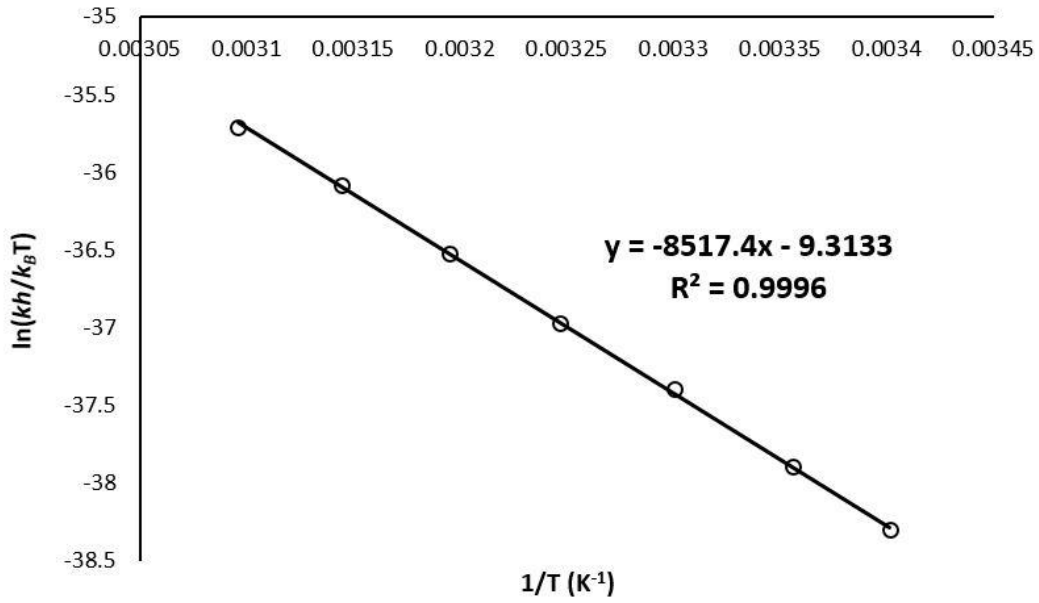

Figure 8. Eyring plot representing the dependence of amide HDX k_{obs} on temperature (guest = PEt_4^+; pD_{corr} 8.40, $\Delta H^{\ddagger}$: 71(1) kJ·mol^{-1}; $\Delta S^{\ddagger}$: -77(2) J·mol^{-1}·K^{-1}).

References

(1) Buch-Pedersen, M. J.; Pedersen, B. P.; Veierskov, B.; Nissen, P.; Palmgren, M. G. *Pflüg. Arch. Eur. J. Physiol.* **2009**, *457* (3), 573.
(2) Nagle, J. F.; Tristram-Nagle, S. *J. Membr. Biol.* **1983**, *74* (1), 1.
(3) Liang, Z.-X.; Klinman, J. P. *Curr. Opin. Struct. Biol.* **2004**, *14* (6), 648.
(4) Fillingame, R. H. *J. Bioenerg. Biomembr.* **1992**, *24* (5), 485.
(5) Akeson, M.; Deamer, D. W. *Biophys. J.* **1991**, *60* (1), 101.
(6) Klinman, J. P.; Kohen, A. *Annu. Rev. Biochem.* **2013**, *82*, 471.
(7) Knapp, M. J.; Klinman, J. P. *Eur. J. Biochem.* **2002**, *269* (13), 3113.
(8) Anderson, J. S.; Hernández, G.; LeMaster, D. M. *Biochemistry (Mosc.)* **2008**, *47* (23), 6178.
(9) Perrin, C. L.; Chen, J.-H.; Ohta, B. K. *J. Am. Chem. Soc.* **1999**, *121* (11), 2448.
(10) Leichtling, B. H.; Klotz, I. M. *Biochemistry (Mosc.)* **1966**, *5* (12), 4026.
(11) Zhang, Z.; Smith, D. L. *Protein Sci.* **1993**, *2* (4), 522.
(12) Englander, S. W.; Mayne, L.; Bai, Y.; Sosnick, T. R. *Protein Sci.* **1997**, *6* (5), 1101.
(13) Skinner, J. J.; Lim, W. K.; Bédard, S.; Black, B. E.; Englander, S. W. *Protein Sci.* **2012**, *21* (7), 996.
(14) Ariga, K.; Hill, J. P.; Lee, M. V.; Vinu, A.; Charvet, R.; Acharya, S. *Sci. Technol. Adv. Mater.* **2008**, *9* (1), 014109.
(15) Kahsar, K. R.; Schwartz, D. K.; Medlin, J. W. *J. Am. Chem. Soc.* **2014**, *136* (1), 520.
(16) Soberats, B.; Sanna, E.; Martorell, G.; Rotger, C.; Costa, A. *Org. Lett.* **2014**, *16* (3), 840.
(17) Oshovsky, G. V.; Reinhoudt, D. N.; Verboom, W. *Angew. Chem. Int. Ed.* **2007**, *46* (14), 2366.
(18) Breslow, R. *Science* **1982**, *218* (4572), 532.
(19) Breslow, R. *Acc. Chem. Res.* **1995**, *28* (3), 146.
(20) Murase, T.; Nishijima, Y.; Fujita, M. *J. Am. Chem. Soc.* **2012**, *134* (1), 162.
(21) Habicher, T.; Diederich, F.; Gramlich, V. *Helv. Chim. Acta* **1999**, *82* (7), 1066.
(22) Houk, K. N.; Leach, A. G.; Kim, S. P.; Zhang, X. *Angew. Chem. Int. Ed.* **2003**, *42* (40), 4872.
(23) Leung, D. H.; Bergman, R. G.; Raymond, K. N. *J. Am. Chem. Soc.* **2008**, *130* (9), 2798.
(24) Wang, L.-Y.; Yang, Y.; Liu, K.; Li, B.-L.; Zhang, Y. *Cryst. Growth Des.* **2008**, *8* (11), 3902.
(25) Lakshminarayanan, P. S.; Suresh, E.; Ghosh, P. *Angew. Chem. Int. Ed.* **2006**, *45* (23), 3807.
(26) Hazra, A.; Kanoo, P.; Mohapatra, S.; Mostafa, G.; Maji, T. K. *CrystEngComm* **2010**, *12* (10), 2775.
(27) Li, Y.; Jiang, L.; Feng, X.-L.; Lu, T.-B. *Cryst. Growth Des.* **2008**, *8* (10), 3689.
(28) Mandal, S.; Castiñeiras, A.; Mondal, T. K.; Mondal, A.; Chattopadhyay, D.; Goswami, S. *Dalton Trans.* **2010**, *39* (40), 9514.
(29) Kurotobi, K.; Murata, Y. *Science* **2011**, *333* (6042), 613.
(30) Wang, X.; Lin, H.; Mu, B.; Tian, A.; Liu, G. *Dalton Trans.* **2010**, *39* (27), 6187.
(31) Yoshizawa, M.; Kusukawa, T.; Kawano, M.; Ohhara, T.; Tanaka, I.; Kurihara, K.; Niimura, N.; Fujita, M. *J. Am. Chem. Soc.* **2005**, *127* (9), 2798.
(32) Massera, C.; Melegari, M.; Ugozzoli, F.; Dalcanale, E. *Chem. Commun.* **2010**, *46* (1), 88.
(33) Caulder, D. L.; Powers, R. E.; Parac, T. N.; Raymond, K. N. *Angew. Chem. Int. Ed.* **1998**, *37* (13-14), 1840.
(34) Zhao, C.; Sun, Q.-F.; Hart-Cooper, W. M.; DiPasquale, A. G.; Toste, F. D.; Bergman, R.

G.; Raymond, K. N. *J. Am. Chem. Soc.* **2013**, *135* (50), 18802.
(35) Janser, I.; Albrecht, M.; Hunger, K.; Burk, S.; Rissanen, K. *Eur. J. Inorg. Chem.* **2006**, *2006* (1), 244.
(36) Zhao, C.; Toste, F. D.; Raymond, K. N.; Bergman, R. G. *J. Am. Chem. Soc.* **2014**, *136* (41), 14409.
(37) Hart-Cooper, W. M.; Zhao, C.; Triano, R. M.; Yaghoubi, P.; Ozores, H. L.; Burford, K. N.; Toste, F. D.; Bergman, R. G.; Raymond, K. N. *Chem. Sci.* **2015**, *6* (2), 1383.
(38) Hart-Cooper, W. M.; Clary, K. N.; Toste, F. D.; Bergman, R. G.; Raymond, K. N. *J. Am. Chem. Soc.* **2012**, *134* (43), 17873.
(39) Pluth, M. D.; Bergman, R. G.; Raymond, K. N. *Acc. Chem. Res.* **2009**, *42* (10), 1650.
(40) Fiedler, D.; van Halbeek, H.; Bergman, R. G.; Raymond, K. N. *J. Am. Chem. Soc.* **2006**, *128* (31), 10240.
(41) Glasoe, P. K.; Long, F. A. *J. Phys. Chem.* **1960**, *64* (1), 188.
(42) Sgarlata, C.; Mugridge, J. S.; Pluth, M. D.; Tiedemann, B. E. F.; Zito, V.; Arena, G.; Raymond, K. N. *J. Am. Chem. Soc.* **2010**, *132* (3), 1005.
(43) Davis, A. V.; Fiedler, D.; Seeber, G.; Zahl, A.; van Eldik, R.; Raymond, K. N. *J. Am. Chem. Soc.* **2006**, *128* (4), 1324.
(44) Davis, A. V.; Raymond, K. N. *J. Am. Chem. Soc.* **2005**, *127* (21), 7912.
(45) Mugridge, J. S.; Bergman, R. G.; Raymond, K. N. *Angew. Chem. Int. Ed.* **2010**, *49* (21), 3635.
(46) Mugridge, J. S.; Bergman, R. G.; Raymond, K. N. *J. Am. Chem. Soc.* **2010**, *132* (4), 1182.

Chapter 5
Conclusion

Over four billion years, the engine of natural selection has tested billions of living designs which transform the surface of our planet. The mechanisms by which life operates rely on the noncovalent associations of biomacromolecules with water and each other. These associations are being discovered and described in the field of aqueous self-assembly. Studies in this field, leading to advances in aqueous supramolecular catalysis, will help to understand the factors that control noncovalent interactions and may also ultimately ensure the environmentally benign chemical use and energy production needed by modern society.

The first two research chapters of this dissertation describe a terpene transformation catalyzed by a synthetic enzyme mimic. Effectively, a fragrant mosquito-repelling component of plant sap turns into the direct precursor of menthol, an antimicrobial pain-reliever. This process exhibited a confounding relationship with solution acidity, which led to fundamental studies of host-mediated proton transfer. After some time and with a great deal of assistance, the author emerged with some understanding of the mechanisms by which an archetypic enzyme mimic exchanges protons with water. Results and interpretation support a proton transfer mechanism that, like the formation of the host itself, confers emergent behavior unique to the integration of its parts. Studies, puzzles and problems involving macromolecule-water interactions will recur with the advancement of biomimetic and sustainable chemistry.

Biomimicry is a design philosophy that can sustainably promote environmental conservation. The design principles of organisms can be distilled into principles benefitting diverse fields, such as architecture and chemistry. If these principles, or benefits thereof, are appreciated by the greater community, species conservation may accumulate a growing valuation. Chemical biomachinery has advanced so that it creates what is conventionally deemed "technology." Biomimetic approaches to supramolecular design may simultaneously enable sustainable chemical use while encouraging protection of the natural environment to which we all belong.

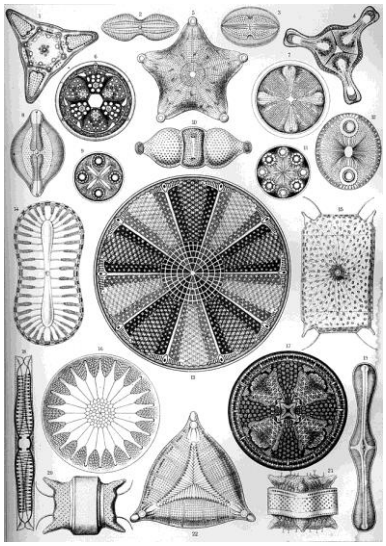

Figure. Unicellular, silica-encrusted diatoms are organisms whose symmetrical forms resemble certain supramolecular polyhedra. Image by Ernst Haeckel, *Kunstformen der Natur*, 1904.